

Aspects of Analyticity

Dieter R. Brill ¹

CONTENTS

- 1 Introduction
- 2 Analytic Manifolds and Analytic Continuation of Metrics
- 3 Walker's Spacetimes and their Maximal Extension
- 4 Global Structure of de Sitter and Reissner-Nordström-de Sitter Cosmos
 - 4.1 Special Cases
 - 4.2 Collapsing Dust
- 5 Euclidean Metrics
- 6 Physical Interpretation of Euclidean Solutions, and a remark about the Gravitational Action
 - 6.1 Thermal Interpretation
 - 6.2 Tunneling Interpretation
- 7 The Multi-Black-Hole Solutions
 - 7.1 Merging Black Holes
 - 7.2 Continuing Beyond the Horizons
- 8 Naked Singularities?
- References

¹ Department of Physics, University of Maryland, College Park, MD 20742, USA

1 Introduction

In these lectures I discuss a number of diverse topics that happen to be related to analyticity and analytic continuation. (This relation allows for a concise title, but otherwise appears superficial — I do not claim to understand its the deeper basis, if any.) I begin with some remarks about the uses and problems of analyticity in spacetime physics. As an illustration of the possibilities I discuss spherically symmetric spacetimes, whose analytic continuation is completely understood. An example, the Reissner-Nordström-deSitter space, is treated with particular attention to extreme cases.

Next I consider a different type of analytic continuation, namely to “imaginary time”, or Euclidean geometries. These may be interpreted physically as thermal states or as tunneling states. As an example I recall the thermal Schwarzschild and Reissner-Nordström solutions, and the question of their entropy. This leads to a discussion of the appropriate gravitational action, and the action associated with sharp corners or “joints” of the boundary. In the realm of tunneling states I give several examples and their physical interpretation, with particular attention to black hole pair creation and universe creation “from nothing.”

Returning to Lorentzian analytic continuation I discuss the dynamical multi-black-hole solutions of Kastor and Traschen. This solution describes a cosmology with several charged black holes in motion and capable of collision. I explore the prospects of continuing the solution beyond the region in which it was originally defined. The spacetime so continued can then contain a naked singularity and provide a counterexample to some versions of the cosmic censorship hypothesis.

2 Analytic Manifolds and Analytic Continuation of Metrics

If we have a spacetime that can be covered by a single coordinate patch, and the metric is an analytic function of those coordinates, then there is usually no problem in extending the metric to the entire spacetime. But interesting applications of Einstein’s equations frequently occur in manifolds of complicated topology, which cannot be covered by a single coordinate system. In that case the region in which an exact solution is first known is typically incomplete. The simplest way to complete it, if possible, is by analytic extension. It is remarkable how little is known in a systematic way about this frequently encountered problem. Here we will not materially improve on this situation, but merely recall some of what is known about analytic continuation, and discuss the most common class of geometries for which a method exists.

It is tempting to expect that one can in general continue analytic solutions (say of the sourceless Einstein equations) beyond their initial coordinate neighborhood. However, we will find that this is not always possible. That is, some solutions that are analytic in one neighborhood and present no obvious obstruction to continuation by way of diverging curvature invariants may nonetheless be only of finite differentiability on the neighborhood’s boundary. There is of course nothing unphysical about such behavior; it is what one expects, for example, in the presence of a gravitational waves pulse of finite spatial extent. The reason it is necessary to extend incomplete spacetimes is because one purpose of spacetime is to describe the history of all inertial observers. A (timelike) geodesically incomplete spacetime fails to do this, so it behooves us to extend it as far as possible. (If even the maximal extension is incomplete we can begin to ask questions about cosmic censorship.) An analytic extension, if it exists, is special because of its uniqueness and “permanence”. The uniqueness is similar to that of the continuation of analytic functions: If the metric is analytic in a neighborhood of an analytic spacetime, then its analytic continuation is unique. If not only the metric but also the manifold needs to be continued, then the continuation is *not* necessarily unique. A simple example is a finite part of (flat) Minkowski space, which can be continued either to the complete Minkowski space, or to one of the several

locally Minkowskian spaces, such as the torus. More generally, any simply connected part of spacetime that can be continued to a multiply connected one can also be continued to a covering of the latter. (We will encounter such ambiguities with cosmological black hole spacetimes in section 4). A somewhat more subtle example is the Taub-NUT space, which has two distinct and inequivalent analytic extensions [2]. In these ambiguous cases one needs to decide on such properties as the topology of the extended manifold along with the extension of the metric. Once the whole (smooth) manifold is known, its analytic structure is essentially unique.

How do we define an analytic manifold? To treat *real* extensions the appropriate notion is real analyticity: a function is analytic if it can be represented locally by a power series expansion. On the other hand, we may want to consider complex extensions, for example to “imaginary time”; in that case we would use the usual notion of analyticity in the complex plane. In either case a manifold is analytic if the coordinate transformations between neighborhoods are (real resp. complex) analytic functions. Tensors are analytic if their components in analytic coordinates are analytic. Of course, in non-analytic coordinates the components will in general not be analytic, even if the tensor itself is.

Suppose we have an analytic differential equation, such as the sourceless Einstein equations, on such a manifold, and a local analytic solution. An analytic continuation of the solution will then also satisfy the (continued) differential equation.² This is the “permanence” property of analytic continuations. It makes such continuations interesting because one gets a “new” solution “for free,” i.e. without having to solve the equation again. But the continuation is not necessarily an easy matter when the metric is given in some coordinates, and we desire to extend across a boundary where both the metric coefficients and the coordinates are non-analytic. There appears to be no systematic criterion for deciding whether analytic continuation is possible, and one usually has to rely on ingenuity to find suitable new coordinates in which the metric is analytic in the relevant region.

It can also happen that neither the metric nor the coordinates are analytic functions on the manifold, but the metric coefficients are analytic functions of the coordinates; or they may be extendable to another (real) range of the coordinates by an excursion in the complex plane. Examples of this are found in the Schwarzschild metric at $r = 2M$ and $r = 0$ respectively. In either case we obtain solutions of the Einstein equations in the new coordinate range, but it is a separate question whether and how the geometry so described fits together with the original geometry, and if so, whether the fit is analytic. Finding a proper overlap seems to be the only way to assure the latter.³ For a class of metrics, which I discuss in section 3, one knows how to fit together the pieces across horizons like $r = 2M$ for the Schwarzschild geometry.

One can, of course, give criteria that establish *non*-analyticity, for example the divergence of invariants formed from the Riemann tensor and/or its derivatives. This happens, for example, at $r = 0$ in the Schwarzschild metric, so no real analytic extension is possible there. But for indefinite metrics not all divergences of the Riemann tensor can be found in this way. Namely, the Riemann tensor may have a “null” infinity, as in $R_{\mu\nu\alpha\beta} = l_{[\mu}m_{\nu]}l_{[\alpha}m_{\beta]}$, with $l^\mu l_\mu = 0$, $l^\mu m_\mu = 0$ and divergence in l, m . In that case the divergence can be found by evaluating the Riemann tensor components in an orthonormal frame. (To avoid spurious infinities due to the frame becoming null the orthonormal frame should be parallelly propagated [18]).

If one admits an excursion to complex coordinate values one may find other real metrics analytically related to the original one. Because there may be other “real sections” of the

²Analyticity is not assured, nor is it necessarily to be expected on physical grounds, if there are source terms present. Well-known examples are stellar models that are non-analytic on the stellar surface.

³It is remarkable that some solutions known in closed form (which is sometimes — loosely — called “analytic”) can be extended with a high degree of differentiability (e.g. C^{122} as in [3]), and in certain of the spaces discussed in section 7) but not analytically.

complex metric, such extensions may not be unique.⁴ Also, they may have nothing directly to do with the original geometry. In fact, the “extension” may have a different signature than the original metric. This is a favorite way to generate Euclidean solutions such as the ones discussed in section 5. An example of a Lorentzian, complex analytic relation of the Schwarzschild metric (which can however hardly be said to be physically related) is

$$ds^2 = \left(1 - \frac{2M}{r}\right) dt^2 + \frac{dr^2}{\left(1 - \frac{2M}{r}\right)} - r^2 d\theta^2 + r^2 \cosh^2 \theta d\phi^2.$$

(This is obtained from the usual Schwarzschild geometry by $t \rightarrow it$, $\frac{\pi}{2} - \theta \rightarrow i\theta$.) Another example is the continuation of the de Sitter space metric,

$$ds^2 = -dt^2 + e^{2Ht}(dx^2 + dy^2 + dz^2)$$

across $t = 0$, which effectively changes the cosmological expansion parameter H into its negative.

Because “new” information can propagate along null surfaces, such surfaces are a natural analyticity boundary. On the other hand, analyticity of a region would be expected to extend to the domain of dependence of that region. Even when the geometry itself can be extended, the coordinates in which a metric is originally found tend to be analytic only in such domains of dependence. One of the few, somewhat general approaches to extend such metrics proceeds by introducing null coordinates in which the boundary is one of the coordinate surfaces. Such is the case in the following class of metrics.

3 Walker’s Spacetimes and their Maximal Extension

The extensions of spherically symmetric “static” metrics of the form

$$ds^2 = -F dt^2 + \frac{dr^2}{F} + r^2 d\Omega^2 \tag{1}$$

have been completely discussed by Walker [5]. Here $F = F(r)$ is the norm of the Killing vector $\partial/\partial t$; it is not required to be timelike (hence the quotes around “static”) because we allow F to be positive or negative. F may be an analytic function of r , satisfying the Einstein equation, and range over positive and negative values, but the metric is clearly non-analytic at the zeros of F ; the problem is to find the continuation across these zeros. (Infinities of F imply infinities of the Riemann tensor, so no analytic continuation is possible there.) Because the angular part is regular for $r > 0$, it suffices to confine attention to the two-dimensional r, t part of the metric.

In this two-dimensional space one can easily introduce null coordinates by “factoring” the metric as a product of two integrable null differential forms,

$$du = dt + \frac{dr}{F}, \quad dv = dt - \frac{dr}{F}. \tag{2}$$

The metric then takes the double null form, $ds^2 = -F(u-v) dudv$, but this is still singular at $F = 0$. If instead, following Finkelstein’s trick, we use r and only *one* null coordinate, say u , the metric assumes the nonsingular form

$$ds^2 = -F(r) du^2 + 2dudr,$$

⁴To restore uniqueness it has been suggested [4] that the slightly complex path should be a geodesic. It remains to be seen whether one does not still lose physical significance in this unorthodox continuation.

which is analytic wherever F is analytic as a function.⁵ This metric, then, provides the overlap necessary to connect two regions with opposite signs of F . How two such regions fit together can be shown by a conformal diagram, as in Fig. 1. Here we have assumed that the region $r \rightarrow \infty$ has the usual asymptotically flat structure, and that there is another zero of F at finite r below $r = a$ (corresponding to the “roof” of the figure). If these structures are different, the blocks may be shaped differently, but the region around the zero, $r = a$, will look the same.

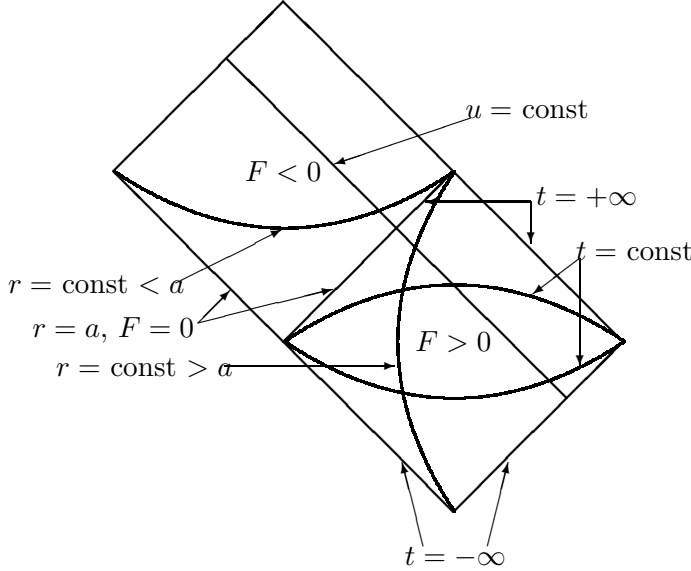


Fig. 1. Conformal diagram of region of Walker metric surrounding $r = a$, the largest zero of F . The r, t coordinates are degenerate on the boundaries of the diamond-shaped regions. For example, along the lower left boundary both t and r are constant (namely $r = a$).

The spacetime as shown is still not complete. For example, the middle left boundary labeled $r = a$ is at a finite distance from typical points inside the region, and so is the “roof.” By using Finkelstein coordinates r and v we obtain a system that overlaps the middle left boundary, and by repeating this procedure around the next smaller zero below $r = a$ we can extend beyond the “roof.” Thus in passing through each zero of F we add several new diamond-shaped regions to the conformal diagram, according as we cross the boundary along $u = \text{const}$ or $v = \text{const}$. All the regions so generated at the zero of F where $r = a$ are shown in Fig. 2.

⁵If F is only smooth or C^n , this provides a smooth or C^n extension across $F = 0$. In those cases the extension is of course not unique.

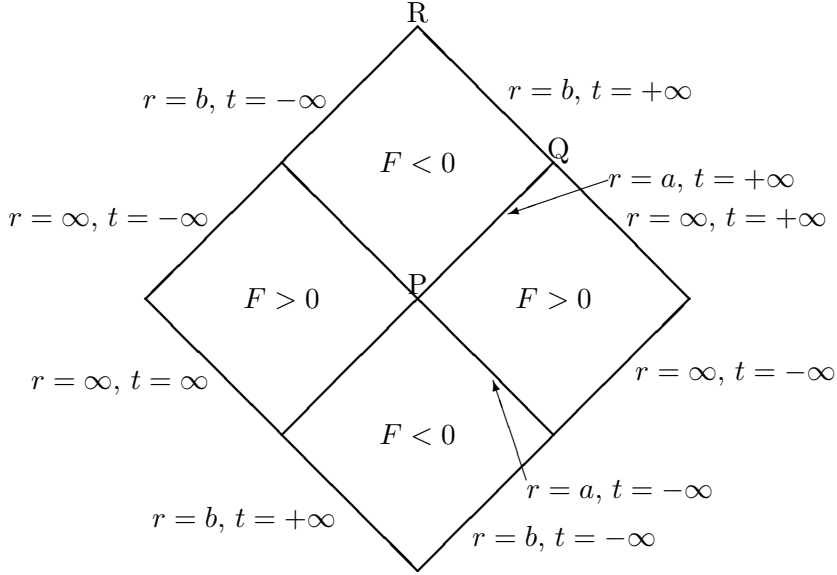


Fig. 2. Blocks that fit together at their $r = a$ boundary. The next lower zero of F occurs at $r = b$.

The four blocks in Fig. 2 are connected across all the diagonal lines, because the overlapping coordinates constructed so far reach across all of these lines. But these coordinates are not good at the intersection points P, Q, R, . . . , so we do not yet know whether the regions fit together at a point like P, where four regions meet. In fact, the intersection points come in two types: those like P and R are characterized by the vanishing of the $\partial/\partial t$ Killing vector, whereas at points like Q different values of r are “trying to come together.” It is therefore not surprising that no analytic continuation is possible or necessary across points of type Q; they lie at an infinite distance ($t \rightarrow \infty$) along Killing orbits and are not part of the manifold.

At points of type P the blocks may fit together smoothly or analytically, depending on the form of F . We cannot analyze point P using the coordinates u or v , because we have $u = -\infty$, $v = \infty$ there. But if we introduce exponentials of these coordinates,

$$U = e^{cu}, \quad V = e^{-cv}$$

where c is a adjustable constant, then (for $c > 0$) $U = 0 = V$ at P and the metric takes the form

$$ds^2 = \frac{F}{c^2} e^{(-2c \int \frac{dr}{F})} dU dV.$$

The trick is now to choose c so that the conformal factor in this expression is finite. It is not difficult to verify that this can be done when F has a simple zero (for example, if $F = r - r_0$ one finds $c = \frac{1}{2}$). For functions F of the type

$$F(r) = \frac{\prod_i (r - a_i)}{K(r)}, \quad (3)$$

with $K(r)$ a polynomial with zeros differing from the a_i , Walker [5] shows that c can be chosen so that the metric becomes regular at P — the four blocks fit together smoothly or analytically.

If two roots coincide, the picture looks different. There are no points of type P because the double-root horizon is at an infinite spatial distance; a spacelike section does not have the “wormhole” shape, but is an infinite funnel or “cornucopion.” Figure 3 shows how the blocks

fit together in that case [6]. All lines and curves that are shown correspond to $r = \text{const}$. This diagram looks like what one would obtain by continuing Fig. 1 towards the upper left by the usual rules to another block with $F > 0$, and then eliminating the $F < 0$ block and moving the two $F > 0$ blocks together. Thus the coincidence limit of two roots of F does not appear continuous in the conformal picture.

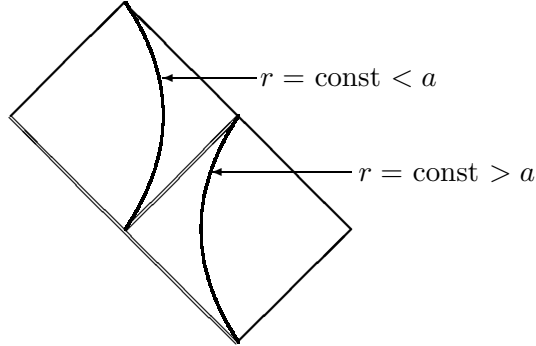


Fig. 3. Conformal diagram of region of Walker metric surrounding a double root of F , denoted by double lines.

This happens, for example, for the Reissner-Nordström geometry. For this case one has

$$F = 1 - \frac{2M}{r} + \frac{Q^2}{r^2} = \frac{(r - r_+)(r - r_-)}{r^2}.$$

The coincidence limit $r_+ \rightarrow r_-$ corresponds to an “extremally” charged black hole, $Q^2 \rightarrow M^2$. As long as the roots are distinct the two $F > 0$ blocks have a finite size $F < 0$ block between them, but at the extremal limit the situation of Fig. 3 applies (except that the upper left block ends at $r = 0$ rather than continuing to another zero of F).

One can also take a different limit, which leads to another solution that has nothing directly to do with the analytic continuation of the first block. Instead of eliminating the $F < 0$ block, one can keep its physical size constant by rescaling the metric: define a and ϕ by

$$2a = r_+ - r_-, \quad a \cos(\phi/a) = r - \frac{1}{2}(r_+ + r_-).$$

For small a the region between the two roots has the metric

$$ds^2 = (a/M)^2 \sin^2 \phi dt^2 - (aM)^2 d\phi^2.$$

The metric ds^2/a^2 is related to the Bertotti-Robinson universe. (More detail on the relation between the extremal Reissner-Nordström and the Bertotti-Robinson geometries is found in [7].)

Beyond the coincidence limit it can happen that a pair of (real) roots disappear. This is also not a continuous change in the conformal diagram — the two regions of Fig. 3 merge into one.

4 Global Structure of de Sitter and Reissner-Nordström-de Sitter Cosmos

The Reissner-Nordström-de Sitter (RNdS) metric for a black hole of mass M and charge Q in a universe with cosmological constant Λ is of type (1), with F of the form

$$F(r) = \frac{\left(-\frac{1}{3}\Lambda r^4 + r^2 - 2Mr + Q^2\right)}{r^2}, \quad (4)$$

which is of the type (3). Thus we know that the maximal analytic extension is given by the Walker construction, and once we know how the blocks fit together we can do all calculations in the original r, t coordinates.

From the above block-gluing rules it is clear that the conformal diagrams for the Reissner-Nordström-de Sitter metrics depend only on the number of zeros of the function F in (4). We will denote the zeros of the numerator, in decreasing order, by $a_1 \dots a_4$. Only three of the roots are positive (for positive M and Λ). The simplest example is de Sitter space itself, $M = 0, Q = 0$, so $a_1 = \sqrt{3/\Lambda}$, $a_2 = a_3 = 0$. The blocks look different in this case, because $r = 0$ is a regular origin. Also, $r = \infty$ is infinite distance in time (since $F < 0$ for $r > a_1$), so we can identify it with timelike and null infinity, \mathcal{I} . Figure 4a shows an embedding of an r, t subspace of this geometry in flat 3-dimensional Minkowski space, and Fig. 4b is the corresponding conformal diagram. Note that the conformal diagram corresponds to only half of the embedded surface, because the latter shows both “sides” of the origin ($\phi = 0$ and $\phi = \pi$, for example).

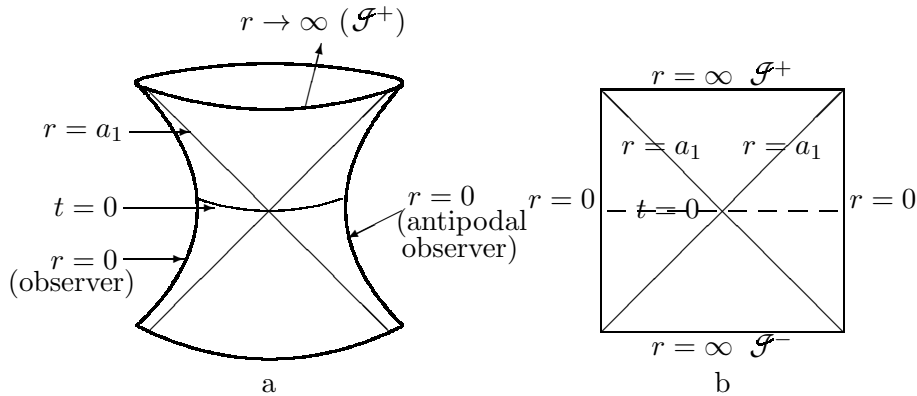


Fig. 4a. Embedding of 2-D de Sitter space in 3-D Minkowski space.

Fig. 4b. The corresponding conformal diagram.

De Sitter space is often described in coordinates different from the r, t used above, in which the space sections are conformally flat. These new coordinates r', t' are called *isotropic* or *cosmological* coordinates [21],

$$r = r' e^{Ht'} \quad t = t' - \frac{1}{2H} \ln(1 - H^2 r'^2).$$

Here $H = \sqrt{\Lambda/3} = 1/a_1$ is the “Hubble constant” or cosmological expansion parameter. The metric then becomes

$$ds^2 = -dt'^2 + e^{2Ht'} (dr'^2 + r'^2 d\Omega^2). \quad (5)$$

These coordinates cover more of de Sitter space than one patch of the r, t coordinates, but there still is a horizon at $t' = -\infty$. Another block of r', t' coordinates but with opposite sign of H can be analytically connected to the original one. We call the coordinates “expanding” in the block with $H > 0$, and “contracting” in the other one. Figure 5 shows some of the spacelike surfaces $t' = \text{const}$.

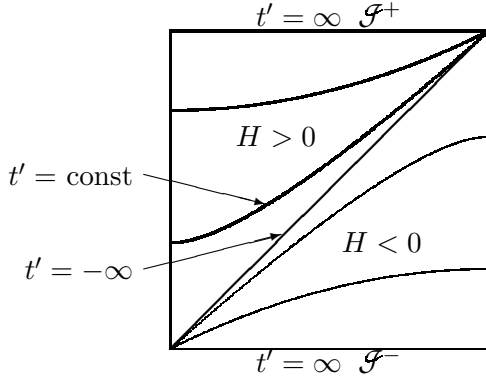


Fig. 5. Cosmological coordinates in de Sitter space. The part drawn in thick lines is the expanding region.

That the de Sitter universe can appear as either static (4), or expanding or contracting (5), is an accident due to the high degree of symmetry of this model. In fact, each “observer” (timelike geodesic) has a static frame centered around him/her. When there is a “single” black hole present, a static frame still exists (but only the one that is centered about the black hole). We will therefore treat the analytic extension of this case by Walker’s method; but we also want to show how the expanding and contracting, cosmological frames fit together (because only their analog exists in the spacetimes [1] with several black holes.)

We rewrite the RNdS metric (4) using capital letters to denote the static frame (in order to distinguish it from the cosmological coordinates, which will be in lower case):

$$ds^2 = -F dT^2 + \frac{dR^2}{F} + R^2 d\Omega^2$$

$$F = 1 - \frac{2m}{R} + \frac{Q^2}{R^2} - \frac{1}{3}\Lambda R^2 \quad A_T = -\frac{Q}{R}.$$

By means of a somewhat involved coordinate transformation [21] one finds the form of the metric in cosmological coordinates,

$$ds^2 = -V^{-2} dt^2 + U^2 e^{2Ht} (dr^2 + r^2 d\Omega^2), \quad (6)$$

where

$$U = 1 + \frac{M}{\rho} + \frac{M^2 - Q^2}{4\rho^2} \quad V = \frac{U}{1 - \frac{M^2 - Q^2}{4\rho^2}} \quad \rho = e^{Ht} r.$$

By means of the simple coordinate change

$$\tau \equiv H^{-1} e^{Ht}$$

we can extend the region covered by these coordinates, by allowing τ to be negative as well as positive. The metric and EM potential then become

$$ds^2 = -\frac{d\tau^2}{U^2} + U^2 (dr^2 + r^2 d\Omega^2) \quad U = H\tau + \frac{M}{r} \quad A_\tau = \frac{1}{U}. \quad (7)$$

Figure 6 shows the analytic extension constructed according to the prescription of Sect. 3 for the generic case, when there are three roots of F .

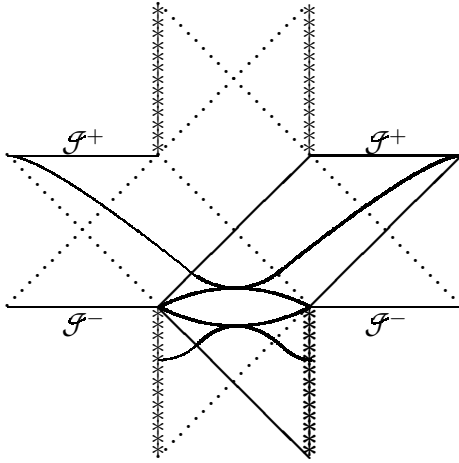


Fig. 6. Conformal diagram of the RNdS geometry. The diagonal (mostly dotted) lines are the horizons corresponding to the three roots of F that separate the different “static” blocks. Those crossing between \mathcal{F}^- and \mathcal{F}^+ are the cosmological horizons at $R = R_c = a_1$; those crossing at the center of the figure are the outer black hole horizons at $R = R_o = a_2$; and those crossing at the top and at the bottom are the inner horizons at $R = R_i = a_3$. The multiply-crossed vertical lines are the singularities at $R = 0$. The thin curves describe surfaces of constant cosmological time τ , the upper one having $\tau > 0$, and the lower one $\tau < 0$. The cosmological r -coordinate is single-valued only to the right (or only to the left) of the point of contact of these curves with the lens-shaped region. This point of contact is a “wormhole throat” of the spacelike geometry. Surfaces of different τ -value touch the lens-shaped region at different points. The boundaries of the lens-shaped region are given by $R = \text{const} = M \pm \sqrt{M^2 - Q^2}$. The two region covered by the right-hand parts of these spacelike surfaces, in which the cosmological coordinates are therefore single-valued, is shown by the thick outlines. Note that the part near \mathcal{F}^+ is similar to that shown in Fig. 5. The lens-shaped region in between is not covered by these coordinates. These regions as drawn are appropriate for expanding coordinates. A region covered by contracting coordinates is obtained, for example, by reflecting the regions in thick outline about the horizontal symmetry axis.

The figure can be repeated indefinitely in the horizontal and the vertical direction, yielding a spacetime that is spacelike and timelike periodic. The spacelike surface $T = 0$ that cuts the figure horizontally in its center then has the geometry akin to a string of beads: its spatial geometry is given by

$$ds^2 = F^{-1}dR^2 + R^2dS^2,$$

which can be embedded in four-dimensional flat space, $dZ^2 + dR^2 + R^2dS^2$ by

$$Z = \int \sqrt{F^{-1} - 1} dR.$$

The surface has maximal radius R_c at the cosmological horizon, and minimal radius R_o at the throats of the holes. The maxima correspond to the large regions of the universe (the “background de Sitter space”), and the minima are throats of wormholes that connect one de Sitter region with the next. Thus each de Sitter region contains two wormhole mouths, placed in antipodal regions of each large universe. (This is the reason for the quotes above when calling this a “single” black hole in a de Sitter universe.) One of these de Sitter regions is shown in Figure 7. Isometric copies of this surface can be smoothly joined at the throats, producing a periodic $S^2 \times R^1$ spatial topology, in which the interiors of the black holes lead to further de Sitter regions.

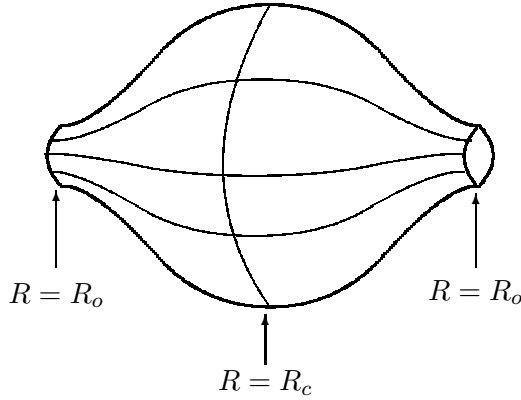


Fig. 7. The geometry of the $T = 0$ slice of Fig. 6, embedded in flat space with a polar angle suppressed. Typical electric field lines are shown.

Alternatively and more compactly we can imagine the left and right halves of the figure identified, so that the horizontal spacelike surface of the figure is a closed circle, and the 3-D spacelike topology is $S^1 \times S^2$. In this case the electric flux of the charge Q also describes closed circles: it emerges from one wormhole mouth, spreads out to the maximum universe size, reconverges on the other mouth, and flows through the wormhole back to the first mouth. Seen from the large universe, the first mouth appears positively charged, and the antipodal one, negatively charged — an example of Wheeler’s [15] “charge without charge”!

4.1 Special cases

The picture of Fig. 6 changes, for example as in Fig. 3, when roots of F coincide or cease to be real (see [21] and [10]). It is easily checked that the quartic $R^2F(R)$ has exactly one negative root, and generically either one or three positive roots, with special cases of double or triple roots. The possibilities for the positive roots are as follows.

- (i) The generic black-hole case: three simple roots $R_c > R_o > R_i$, as in Fig. 6. There are three types of Killing horizon: cosmological horizons at $R = R_c$ and inner and outer black-hole horizons at $R = R_i$ and $R = R_o$ respectively.
- (ii) The generic naked-singularity case: one simple root, giving only cosmological horizons (as in Fig. 9).
- (iii) The extreme (or “cold”) black-hole case: a double root R_d and a simple root $R_c > R_d$, corresponding to a degenerate black-hole horizon at $R = R_d$ and a cosmological horizon at $R = R_c$.
- (iv) The extreme (or marginal) naked-singularity case: a double root R_d and a simple root $R_i < R_d$, corresponding to a degenerate cosmological horizon at $R = R_d$ and an inner horizon at $R = R_i$.
- (v) The “ultra-extreme” case: triple root, with one doubly degenerate horizon.

To make explicit which case occurs for each (M, Q, Λ) , we note that the double roots occur if and only if $M = M_{\pm}(Q, \Lambda)$, where

$$M_{\pm} = P_{\pm} \left(1 - \frac{2}{3} \Lambda P_{\pm}^2 \right), \quad P_{\pm}^2 = \frac{1}{2\Lambda} \left(1 \pm \sqrt{1 - 4\Lambda Q^2} \right),$$

with the double root being at $R = P_{\pm}$ [16]. The ultra-extreme case occurs when $9M^2 = 8Q^2 = 2/\Lambda$, so that $P_+ = P_-$. Otherwise, the extreme black hole occurs if $M = M_-(Q, \Lambda)$, and the extreme naked singularity occurs if $M = M_+(Q, \Lambda)$. The generic black hole occurs if $M_-(Q, \Lambda) < M < M_+(Q, \Lambda)$, and the generic naked singularity otherwise.

A constant- T spatial surface of the generic naked-singularity solution has topology $S^2 \times R^1$, which can be visualized as an S^3 punctured at opposite poles, with the two singularities being at finite affine distance. The electric field lines diverge from one pole and converge on the other, so that the singularities have the appearance of point charges.

We now turn to the extreme cases. The extreme black-hole solution can be interpreted as a pair of oppositely charged extreme Reissner-Nordström black holes at opposite poles of a de Sitter cosmos. Note that for $\Lambda > 0$ the extreme case occurs for $M^2 < Q^2$. That is, in the cosmological context, the maximal charge on a black hole—beyond which there is a naked singularity instead—is larger than in asymptotically flat space [16], cf. citeBA). The topology of a constant- T spatial surface is $S^2 \times R^1$. The two minimal-radius spheres, which also represent the black holes' horizons, are located at infinite affine distance on this spatial surface, preventing a wormhole identification, so that these black holes are horns rather than wormholes.

The extreme naked-singularity case has a novel structure that suggests the creation and subsequent annihilation of a pair of point charges. A constant- T spatial surface has topology $S^2 \times R^1$, which again can be visualized as an S^3 punctured at opposite poles, with the two singularities being at finite affine distance, and the electric field lines diverging from one pole and converging on the other. Unlike the generic naked singularities, or that of the negative-mass Schwarzschild solution, these singularities do not exist for all time, but develop from an initially regular state, i.e. there are partial Cauchy surfaces, of topology $S^2 \times R^1$ or $S^2 \times S^1$, depending on the identifications made. The singularities are not even weakly censored, in the sense that any observer whose future life is long enough will see them: any path from ι^- to ι^+ passes through the causal future (and the causal past) of the singularities. This is in distinction to the generic black hole, or the Reissner-Nordström black hole, whose singularities remain unseen by wary observers. Another novel feature is that the singularities subsequently dissolve, with the process being visible from \mathcal{F}^+ .

Finally, we note that the ultra-extreme case is similar to the generic naked-singularity case, except that the singularities are at infinite affine distance.

Another special case is of interest here (it can be generalized to include more than two black holes), namely $Q^2 = M^2$. In the RN case this is the extremal black hole, but when $\Lambda \neq 0$ this choice does not force a double root — the global structure and conformal diagram of Fig. 6 still apply. What does change is the way the cosmological coordinates cover the diagram: the lens-shaped region degenerates into the line $\tau = 0$, so that a continuous region between the singularity and \mathcal{F}^+ is covered. Therefore in this case the entire analytic extension of the metric (6) can be obtained by gluing together alternate copies of expanding and contracting cosmological coordinate patches. Figure 8 shows a pair of such regions, with the contracting one outlined by thick lines. (For easy comparison with Fig. 6 it may help to turn the latter upside down.) We see that the expanding patch contains \mathcal{F}^+ , and the contracting one contains \mathcal{F}^- . It is therefore not immediately clear, if we calculate in contracting coordinates only, how to identify the black hole event horizon as the boundary of the past of \mathcal{F}^+ . We can follow outgoing light rays to $r = \infty$, but at that point their geometrical distance R , measured by the Schwarzschild coordinate R (or by the area of the sphere $r = \text{const}$) is still finite, $R = R_c$. However, there is this difference between such light rays and those that fall into the black hole, that the latter reach the geometrical singularity, which *is* contained in the contracting cosmological coordinates. Furthermore, timelike geodesics heading toward the point S in the figure have an infinite proper time. Thus S is a safe haven for observers who desire to avoid the black hole, and it can be regarded as a small piece of \mathcal{F}^+ that can be asymptotically reached in contracting cosmological

coordinates, just enough to be able to identify the event horizon.⁶

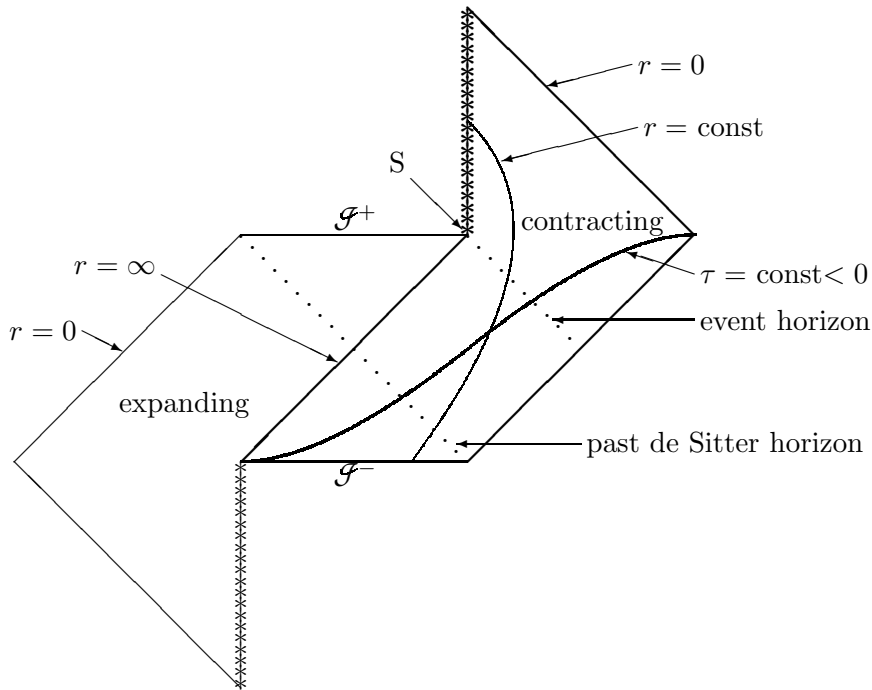


Fig. 8. Two patches of cosmological coordinates for the RNds geometry for the case $Q^2 = M^2$ and $p < 1$ (“undermassive”).

The $Q^2 = M^2$ RNds geometries still depend on two parameters, M and Λ resp. H . A generic black hole occurs if $\Lambda M^2 < 3/16$, an extreme naked singularity if $\Lambda M^2 = 3/16$, and a generic naked singularity if $\Lambda M^2 > 3/16$. The extreme black hole does not occur in this class. If $\Lambda M^2 \ll 1$ the Killing horizons are located approximately at

$$R_i \sim M - HM^2, \quad R_o \sim M + HM^2, \quad R_c \sim H^{-1} - M.$$

(for higher order of approximation see Romans [16].) Stated in terms of the dimensionless parameter $p = 4M|H|$, if $p < 1$ we have the generic black hole or “undermassive” case. If $p > 1$ there is only one real root of $F(R) = 0$. In this generic nakedly singular or “overmassive” case the outer black hole horizon and the de Sitter horizon have disappeared, only what used to be the inner black hole horizon remains. One could also interpret the remaining horizon as a cosmological one, separating the two naked singularities at antipodal regions of a background de Sitter space. The conformal diagram for this case, constructed according to the block gluing rules, is shown in Fig. 9.

⁶This feature holds for the generic case, but is particularly valuable for the multi-black-hole solutions of Section 7.

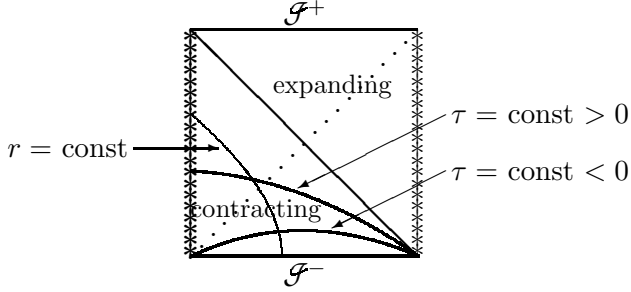


Fig. 9. Two patches of cosmological coordinates for the RNdS geometry for the case $Q^2 = M^2$ and $p > 1$ (“overmassive”). The thick outline shows the contracting patch.

4.2 Collapsing Dust

The solutions discussed so far correspond to “eternal” black holes (or a combination of white holes and black holes). The future part of the usual black hole geometry can be generated from matter initial data, say by the collapse of a sphere of dust. A similar process is possible for $Q^2 = M^2$ RNdS. It is of interest here because the dust can “cover up” an initial black hole singularity, and will be used for that purpose in section 7.

To generate such a geometry from dust, the dust must itself have $Q^2 = M^2$, so that electrical forces largely balance gravitational forces. The dust can still collapse if it has the right initial velocity. A simple situation is dust that is at rest in cosmological coordinates: in any metric and potential of form (6), for an arbitrary U , such dust remains at rest ($r = \text{const}$), if considered as test particles. A typical worldline is shown in Fig. 8. To understand why it behaves this way we look more closely at the electric field associated with this geometry. We know that the parameter Q of the black hole on the left is opposite to that of the one on the right. Suppose the left hole is negative and the right one positive. On the spacelike surface corresponding to a horizontal line drawn through the center of Fig. 8, the electric field will then point from right to left. By flux conservation, the electric field will therefore also point to the left in the region near the upper singularity shown in the Figure. Thus we can associate a *negative* charge with this singularity. (The singularity to the right of the $r = 0$ inner horizon, which is not shown in the Figure, correspondingly has positive charge). The dust particle on the $r = \text{const}$ trajectory has the same charge as the black hole that is included in that coordinate patch, namely positive. It therefore ends up on the negative singularity.

Any point in Fig. 8 can be considered to be in either of two possible cosmological coordinate patches. For example, a point near \mathcal{F}^- is in the contracting patch shown, which contracts about the right black hole. By reflecting this patch about a vertical line through the center of the Figure we obtain a patch that contracts about the left black hole. It also contains the region near \mathcal{F}^- . Its radial coordinate will be denoted by r' . The trajectory $r' = \text{const}$, obtained by reflecting the $r = \text{const}$ trajectory shown in the Figure, describes a negative test charge that falls into the positive singularity of the left (negative) black hole. Similarly the region between the de Sitter and the event horizon in the contracting patch has trajectories of positive charges that fall into the positive black hole, and of negative charges that go to \mathcal{F}^+ . The region inside the event horizon has trajectories that go to one or the other singularity, depending on their charges. Of course all these trajectories that are simply described by $r = \text{const}$ or $r' = \text{const}$ satisfy special initial conditions — their initial position is arbitrary, but their initial velocity is then determined.

To take into account the effect of the dust *on* the metric and potential, one needs to match the vacuum region to an interior solution. For spherical symmetry the matching conditions are equivalent to the demand that the dust at the boundary of the interior region move on a test particle path of the vacuum region. Thus a possible boundary for a collapsing (expanding) ball of dust is $r = \text{const}$ in collapsing (expanding) cosmological coordinates. The surface area $4\pi r^2 U^2$ of the dust ball collapses to zero when $U = 0$, which is also the location of the geometrical singularity; at that point the center of the dust ball must coincide with the surface. The corresponding conformal diagram therefore looks as shown by the thick curves in Fig. 10. The region filled with dots denotes the location of the dust.

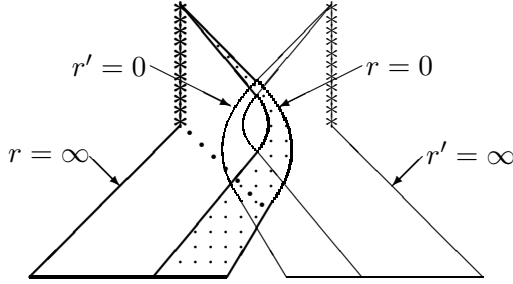


Fig. 10. Conformal diagram for a RNdS black hole generated by the collapse of a ball of charged dust in a de Sitter background (thick lines). The dust region is shown dotted. The dotted line is the black hole event horizon. The thin lines show a dust ball that is symmetrically placed at the antipodal region of the RNdS background, and has opposite charge. If both dust balls are present only the region between the curves $r = 0$ resp. $r' = 0$ applies.

Because the dust includes the origin $r = 0$, there is now no continuation to the right of the heavily outlined region necessary or possible. There is still a cosmological horizon, $r = \infty$, and the continuation on the other side could be analytic (a semi-infinite “string of beads”) or reflection-symmetric about a vertical axis through \mathcal{F}^- (a collapsing dust ball at the antipodal region). Of the two geometrical singularities associated with one RNdS black hole, the dust covers up only the one that would have been on the right in the figure, with the same total charge as that of the dust. The other singularity could be covered up by another dust ball, with the opposite charge. This is shown by the thin curves in Figure 10. If both dust spheres are present, then the physical part of the geometry lies between the $r' = 0$ curve on the left and the $r = 0$ curve on the right. If conditions are as shown, they uncover and then cover up again a (small) region of vacuum RNdS geometry between them.

5 Euclidean Metrics

Complex analytic continuations of a spacetime metric can change the metric’s signature. The new metric will solve the same (analytic) equations (e.g. sourceless Einstein, Einstein-Maxwell, etc) as the original metric. This is most frequently used to obtain positive definite or “Euclidean” solutions of the Einstein equations. Such a continuation will embed the original spacetime in a higher-dimensional space with a complex metric, and the change to a Euclidean metric can be thought of as a rotation from the original, Lorentzian section to the final, Euclidean one. At fixed points the rotation acts also as a rotation on the tangent spaces, and it is clear that the desired change in signature typically leaves a 3-dimensional (real) subspace invariant. Therefore two sections with a real metric typically intersect in a 3-dimensional hypersurface. This hypersurface

will be time-symmetric. In time orthogonal coordinates the metric coefficients will therefore be even functions of the time coordinate, and the continuation is simply described by the familiar replacement $t \rightarrow it$.

Thus any time-symmetric analytic geometry has a Euclidean continuation. The best known Euclidean metrics are obtained from the even simpler case when there is not only the discrete time-symmetry, but also a timelike Killing vector, which must then be orthogonal to the surface of time symmetry; in other words, the original spacetime is static. We consider a few of these cases with particular regard to their global structure.

The Euclidean partner of Minkowski space is of course flat Euclidean space: rectangular coordinates x, y, z, t are a time-symmetric description, and hence suitable for this extension via $t \rightarrow it$.⁷ One can think up many other coordinates in which the replacement works, with the same result (but with different physical interpretation). One is the ‘‘Rindler frame’’, with the metric

$$ds^2 = -x^2 dt^2 + dx^2 + dy^2 + dz^2 \quad (x \geq 0). \quad (8)$$

Here the replacement $t \rightarrow it$ yields Euclidean space in cylindrical coordinates, provided that the Euclidean t -coordinate, which plays the role of the angle variable, has the correct periodicity 2π . (If the periodicity were not right, the Euclidean space would not be regular at the origin, but have a conical singularity there.)

A periodicity is forced on the Euclidean ‘‘time’’ coordinate whenever the Lorentzian metric can locally be put in the form of Eq (8). This will typically happen along a (2-dimensional) ‘‘axis,’’ but there may be more than one such axis. In that case the Lorentzian metric can be regular on both axes, but not the Euclidean metric — unless the periodicities of t required for regularity happen to agree at both places. We will see an example of this in de Sitter space.

The Schwarzschild geometry, being static, also has a Euclidean partner. Because it takes the form of Eq (8) near the horizon, the Euclidean time must be periodic. This is easily seen in the metric’s isotropic form,

$$ds^2 = -\left(\frac{r - M/2}{r + M/2}\right)^2 dT^2 + \left(1 + \frac{M}{2r}\right)^4 (dr^2 + r^2 d\Omega^2).$$

Near the horizon, $r = M/2$, this has the form (8) with $4(r - \frac{M}{2}) = x$, $t = T/4M$, and $16M^2 d\Omega^2 \sim dy^2 + dz^2$. In the Euclidean version, then, t must have periodicity 2π , hence T will have periodicity $8\pi M$.

Because Euclidean space has no conformally invariant lightcones and no \mathcal{G}^\pm , a conformal representation of such spaces is not as revealing as an embedding in a flat higher-dimensional space. Two-dimensional subspaces of interest can often be embedded in flat 3-dimensional space. This is the case for the r, t section of the Euclidean Schwarzschild geometry. In Schwarzschild coordinates embedded in flat space cylindrical coordinates (with T the angle) we have

$$\left(1 - \frac{2M}{R}\right) dT^2 + \left(1 - \frac{2M}{R}\right)^{-1} dR^2 = \rho^2 dT^2 + d\rho^2 + dx^2$$

hence $\rho^2 = \left(1 - \frac{2M}{R}\right)$ and $dx^2 = ((1 - \rho^2)^{-4} - 1) d\rho^2$ specifies the curve whose figure of rotation gives the embedded surface. (Here we have put $4M = 1$ to achieve the proper periodicity, which means that the figure is smooth at its tip.) This embedding is shown in Fig. 11.

⁷It is amusing to contemplate that today we can describe Euclidean space via ‘‘imaginary time’’ in Minkowski space, whereas Minkowski was describing his space by an imaginary coordinate of Euclidean space!

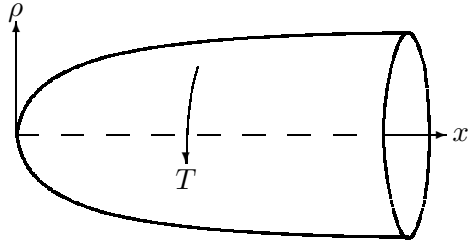


Fig. 11. Embedding of the R, T section of the Euclidean Schwarzschild solution in flat 3-dimensional space.

We see that the *topology* of this surface is \mathbf{R}^2 , and that of the 4-dimensional space is $\mathbf{R}^2 \times \mathbf{S}^2$. However, asymptotically the geometry is cylindrical ($\mathbf{R}^1 \times \mathbf{S}^1 \times \mathbf{S}^2$). Other asymptotically flat Euclidean black hole metrics, obtained e.g. from $t \rightarrow it$ in the RN geometry, result in similar figures. In each case the Euclidean metric extends down only to the r -value corresponding to the outermost horizon, and the horizon itself is the single point on the axis of rotation. One might ask, how can electric field lines point radially outward at infinity without being singular somewhere in Fig. 11? Here it helps to recall that the electric field is a 2-form, it is proportional to the area 2-form of the Figure. As the only boundary of that area is the circle drawn at large x , so there can be electric flux at infinity without another surface for that flux to come from. Similarly, a magnetic charge would be proportional to the area form of the spherical, orthogonal space (which is not shown in Fig. 11).

The embedding looks different for the extreme cases (e.g. $Q^2 = M^2$): the “point on the axis” is infinitely far away, so the surface comes to an infinitely long “spike” of ever-decreasing radius, *if* Euclidean time is given periodic identification (Fig. 12). But because the point on the axis is never reached, there is no conical singularity to be avoided, and no unique period necessary for regularity. In fact, the Euclidean T can equally well have infinite range in that case.⁸

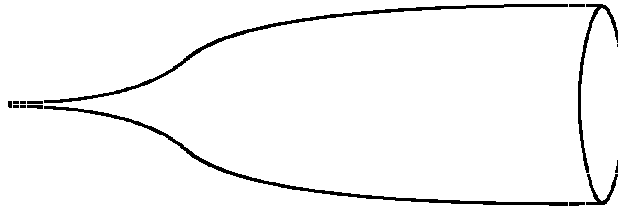


Fig. 12. Embedding of the R, T section of the Euclidean extremal Reissner-Nordström solution in flat 3-dimensional space. The coordinates are similar to those in Fig. 11. The embedding is given by $dx^2 = (\rho^{-2}(1 - \rho)^{-4} - 1) d\rho^2$. The periodicity of T was assumed to be 2π , but this is not necessary. T can have any periodicity, or no periodicity at all. The latter case corresponds to the universal covering space of the Figure.

The Euclidean continuation of de Sitter space is quite simple. Since the curvature is positive constant, the Euclidean partner is the round 4-sphere. One can verify this e.g. in the static frame or in the usual ‘hyperbolic’ de Sitter coordinates. The Euclidean static frame describes

⁸It may be that not all of these are quantum mechanically stable: in the corresponding flat space case, any finite period (“hot flat space”) is unstable.

the R, T subspace (which is a round 2-sphere) in terms of equal-area coordinates.⁹ In hyperbolic de Sitter coordinates, the line element is

$$ds^2 = 3\Lambda^{-1}(-d\theta^2 + \cosh^2 \theta d\mathcal{O}^2),$$

where $d\mathcal{O}^2$ denotes the line element on the round 3-sphere. When $\theta \rightarrow i\theta$ these coordinates become the usual Euclidean polar coordinates on the 4-sphere (except that θ is measured from the equator rather than from the pole). In either case the Euclideanized coordinate (T resp. θ) must have a well-defined period to make the continuation nonsingular. The cosmological coordinates (Eq 5) are not time-symmetric and therefore do not yield a Euclidean section by $t \rightarrow it$, unless we also change H into iH . This implies $\Lambda \rightarrow -\Lambda$, so we would get the Euclidean partner of anti-de Sitter space.

The static part of the RNdS metric (between the outer black hole horizon R_o and the cosmological horizon R_c) can also be continued to Euclidean time. Each horizon requires a periodicity. To find this for a metric of type (1), we expand $F(R)$ around one of its zeros (where R has the horizon value R_H), letting $R - R_H \equiv z^2$:

$$F(R) = F'(R_H)z^2 + \dots \quad dR^2 = 4z^2(dz)^2$$

so that the metric becomes

$$ds^2 \approx F'z^2 dT^2 + \frac{4dz^2}{F'} + R_z^2 d\Omega^2 = \frac{4}{F'} \left(z^2 d(F'T/2)^2 + dz^2 \right) + R_z^2 d\Omega^2.$$

Therefore $z, F'T/2$ are polar coordinates regular at the origin if $|F'|T/2$ has period 2π , or T has period $4\pi/|F'(R_H)|$. For Schwarzschild this yields the well-known periodicity $T_0 = 8\pi M$, as we already found above. For the RNdS solution one finds that the periods required by the two horizons are equal when $Q^2 = M^2$; the period then has the value $T_0 = 2\pi/H\sqrt{1-4MH}$.

There is another special case of RNdS where one can have equality of periods. We saw that the extremal horizons do not require any particular periodicity when Euclideanized. Hence when the inner and outer black hole horizons coincide (see Section 4.1), we can simply assign them the periodicity of the cosmological horizon and thus obtain a regular Euclidean geometry.

An embedding of the R, T subspace of the non-extremal Euclidean RNdS space looks similar to Fig. 11, except that instead of being asymptotically cylindrical, the surface is closed off on the right by a nearly hemispherical cap whose center is the cosmological horizon; the topology of the 4-dimensional space is therefore $S^2 \times S^2$. The extremal case would be shown by Fig. 12 similarly modified.

Flat 3D space cannot, of course, portray more than these two-dimensional subspaces (and the analogous r, ϕ subspaces that are the same as in the Lorentzian geometries). To show, say, the ϕ -direction and fix only θ at $\pi/2$ one would need another independent axis of rotation. But the x -coordinate in Fig. 11 does not differ by more than a factor of 2 from $R - 2M$. We can therefore get an approximate idea of the 3-geometry at the fixed θ by rotating the figure about a vertical axis at distance $2M$ from $x = 0$. Each point in 3-space between the vertical limits of the figure is covered twice (by the front and by the back of the surface) except the points swept out by the vertical section of the figure. Thus one obtains two copies of this region, sown together at their boundaries. The $T = \text{const}$ line on Fig. 11 that represents its section by a vertical plane sweeps out the most geometrically accurate rendition of the R, ϕ subspace: it has the familiar ‘‘wormhole’’ shape.¹⁰ If one confines attention to half the space, which is covered

⁹These are obtained by projecting the 2-sphere (when embedded in 3-space) at constant latitude onto a cylinder that is tangent to the 2-sphere at its equator.

¹⁰It is not quite geometrically accurate, because Fig. 11 is not a paraboloid, whereas the R, ϕ subspace is generated by rotating the Flamm parabola.

once during the rotation, say be the front half of the surface in Fig. 11, then all the $T = \text{const}$, R , ϕ subspaces seem to end at the horizon, except the one generated by the vertical cut. The other surfaces of course do not stop either, but can be smoothly continued into the other half of the space (generated by the back part of the surface).

The same construction applied to RNdS yields the half space shown in Fig. 13. Again the geometry of the outermost $T = \text{const}$ surface is fairly accurately represented. It is the same geometry as that of a $T = \text{const}$ surface in Lorentzian RNdS, namely Fig. 7. (You have to rotate Fig. 7 by 90° and flip the two funnels to the inside so the circles $R = R_o$ can be identified.)

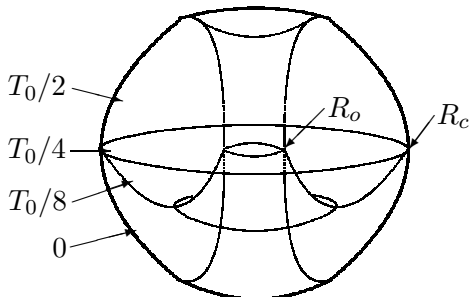


Fig. 13. Half of the 3D subspace $\theta = \pi/2$ of Euclidean RNdS looks like a cored apple. To get the complete subspace, imagine another cored apple identified with the first one everywhere along its surface (including the cored “tunnel”). Here $Q^2 = M^2$ so that the space is regular at both horizons. The cosmological horizon is the outer “equator,” and the black hole horizon is the “inner equator.” The outer surface of the figure plus the tunnel surface corresponds to constant values of T ($T = 0$ and $T = T_0/2$). Two other surfaces of constant T are shown, cutting through the interior of the cored apple, and intersecting each other at the horizons. The intrinsic geometry of all these surfaces is the same, but only the one at $T = 0$ gives a somewhat accurate rendition of its intrinsic geometry.

The same method, using a surface of symmetry, allows us to go from a Euclidean solution back to a Lorentzian one. If the Euclidean space has several symmetries, we do not necessarily have to go back to the Lorentzian space we may have started from. This happens, for example, if we make a Lorentzian continuation “across” the equatorial symmetry plane of the Euclidean Schwarzschild solution. T then remains spacelike (and periodic), but θ becomes timelike. The result is the metric mentioned in Section 2. Although this metric has timelike Killing vectors in any region (just as there is a Killing vector on the sphere that agrees with $\partial/\partial\theta$ at any one point except the poles), it is globally dynamical — it resembles the de Sitter universe in that respect. So one Euclidean solution can be the partner of several Lorentzian ones.

6 Physical Interpretation of Euclidean Solutions, and a remark about the Gravitational Action

Now that we know all about Euclidean solutions of the Einstein equations, what are they good for? We are familiar with analytic extensions into the complex for convenience of calculation or to define quantities that are otherwise not well defined. Similarly, Euclidean spacetimes can be regarded as an elaborate “change of contour.” Such a change is appropriate in connection with thermal states and with tunneling states, and these are indeed the two important ways of using Euclidean geometries. One can take a point of view that does not regard these two ways as different, but frequently the distinction makes sense. For example, as a continuation of the ordinary Schwarzschild solution, the Euclidean Schwarzschild solution is the arena for thermal states; as a continuation of the dynamical metric of Section 2 it is most reasonable

as a tunneling state. On the other hand, the Euclidean continuation of the RNdS solution can have either interpretation. There are interesting unsolved questions connected with these interpretations. For example, in the thermal context there are questions about the source of black hole entropy, the entropy value of extremal black holes, and the “information puzzle.” In the realm of tunneling one would like a better understanding of the boundary conditions, and of the theory that is being approximated. I will not address these unsolved problems, but confine attention to a few simple examples.

6.1 Thermal Interpretation

The connection between periodicity in imaginary time and finite temperature is well known [19]. When the background is periodic Euclidean with period T_0 , only states with (inverse) temperature $\beta = \hbar/kT = T_0$ have finite stress-energy. Any field in the Schwarzschild background at equilibrium should therefore acquire the temperature $\beta = 8\pi M$. This agrees with the Hawking temperature at which the black hole itself radiates. Similarly the periodicity of imaginary Rindler time (Eq 8) corresponds to the temperature seen by accelerated observers.

In a WKB-type approximation to the sum over histories expression for the partition function the most important contribution comes from the classical (Euclidean) action I . When the Euclidean space has a finite size in the T -direction the action of the background space itself is finite and contributes to the free energy and entropy.¹¹ What is the Euclidean black hole action? The Hilbert action, $\frac{1}{16\pi} \int \mathcal{R} dV$, vanishes for any solution of the sourceless Einstein equations (because they imply $\mathcal{R} = 0$, where \mathcal{R} is the curvature scalar). But in order that the action be properly additive in the path integral one must add a surface term to the Hilbert action. The surface term is $-\frac{1}{8\pi} \int K d\Sigma$, where Σ is the surface and K the trace of its extrinsic curvature. With this term the action has the opposite problem from before, it is infinite (because K falls off only as $1/r$ even in flat space, but $d\Sigma$ increases as r^2). One therefore subtracts the flat space contribution, $\frac{1}{8\pi} \int K_0 d\Sigma$, where K_0 is the extrinsic curvature of Σ when embedded in flat space.¹²

For the Euclidean Schwarzschild black hole this action is easily computed: at large R we have

$$K = \frac{2}{R} - \frac{M}{R^2}, \quad K_0 = \frac{2}{R} \quad \text{so} \quad I = -\frac{1}{8\pi} \int_{T=0}^{8\pi M} (K - K_0) d\Sigma = 4\pi M^2. \quad (9)$$

If $\exp(-I/\hbar)$ is the main contribution to the partition function $Z = \exp(-\beta F)$, we have $F = I/\hbar\beta$. Setting $\hbar = 1 = k$ (in addition to $G = 1 = c$ as we have all along) to express all quantities in Planck units we find the value of the free energy $F = \frac{1}{2}M$. If the black hole had no entropy we would expect $F = M$, so the contribution of the entropy is $-\mathcal{T}S = -\frac{1}{2}M$, and since $\mathcal{T} = 1/\beta = 1/8\pi M$ we find $S = 4\pi M^2$. This is usually attributed to the horizon. How can we associate free energy and action with the Euclidean horizon, which is just one point in the R, T surface?

Several ways have been proposed. To find $S = \beta^2 \partial F / \partial \beta$ we need to know how the action changes with β ($= T$). If we change β by changing the periodicity but not the local geometry outside the horizon, we would introduce a conical singularity at the horizon. The tip of the cone

¹¹Existence of gravitational and other degrees of freedom apparently does not change this value of the black hole entropy. This is the “species problem.” The explanation may be that existence of additional species of field changes the renormalization of the gravitational constant to compensate.

¹²Not every Σ can be embedded in flat space, the definition really works only for asymptotically flat (or deSitter, see [14]) spaces in the limit of Σ becoming asymptotic as well. The corresponding prescription in Lorentzian spacetimes works only for boundaries that consist of spacelike and timelike parts meeting orthogonally, and the correction is to be applied only to the timelike parts of the boundary. We do not know any less ad-hoc definition of the action that still gives a finite black hole action for finite (Lorentzian) times.

can be considered to have a δ -function scalar curvature \mathcal{R} . Its contribution to the Hilbert action gives the correct β -dependence to I . Alternatively we can keep the surface regular, but consider how the action is built up out of small steps in β starting from $\beta = 0$ (Fig. 14). A change by $d\beta$ changes the action by that of a wedge of angle $d\alpha = 2\pi(d\beta/8\pi M)$. Because now $\mathcal{R} = 0$ everywhere on this regular surface, the action of the wedge is again due only to the boundary. The large parts of the boundary have $K = 0$, so there is no contribution from them. The short boundary $d\beta$ at infinity contributes, as in Eq (9), $\frac{1}{2}Md\beta$. But now there is also a contribution from the horizon because of the sharp corner there — a δ -function in K . When β and α have reached the value where the whole surface is covered ($\alpha = 2\pi$), all the finite boundaries must cancel. For an arbitrary β the horizon contribution is therefore

$$-\frac{1}{8\pi} \int K d\Sigma = \frac{1}{8\pi} ((\alpha - 2\pi) \times (\text{area of horizon})) = \frac{1}{2}M\beta - \frac{1}{4}A,$$

where $A = 16\pi M^2$ is the area of the horizon. The total action is the sum of the horizon and the asymptotic contributions,¹³

$$I = M\beta - \frac{A}{4}.$$

Now $F = I/\beta = M - A/4\beta$ and $S = \beta^2 \partial F / \partial \beta = A/4$. So we get the same value as before, but with a better understanding why the horizon area enters (it is just the extent of the horizon in the two directions *not* shown in Fig. 14).

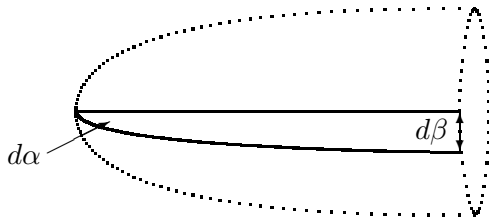


Fig. 14. A change in period by $dT = d\beta$ changes the action by the amount enclosed in the heavy lines. Because these are $T = \text{const}$, $K = 0$ surfaces, the change in the action is due only to the boundary $d\beta$ at infinity, and to the sharp corner of angle $d\alpha$ at the horizon.

We note that a similar picture allows us to interpret the black hole entropy as entanglement entropy: if we propagate only half way around, to $\beta = 4\pi M$, then the beginning and ending surfaces fit together smoothly and have the geometry of a $T = 0$ surface in a (Lorentzian) Schwarzschild wormhole. The Euclidean surface enclosed has no other boundary, it is therefore the WKB approximation to the Hartle-Hawking “no boundary” state of the wormhole. Putting two such “half way around” surfaces together to the full surface of Fig. 11 amounts to (1) tracing over $\beta = 4\pi M$, i.e. the unobserved “interior” part of the wormhole (2) tracing over $\beta = 0$ to get the entangled partition function from the propagator. Thus the entanglement entropy is the same as what we computed above.

In this derivation an important role was played by the action due to a sharp corner or “joint” of the boundary. Such corners are common in Lorentzian regions of integration for the action, typically when spacelike and timelike surfaces meet at right angles. In that case one usually assumes that there is no contribution from such joints. That this assumption is correct (but not for other angles, i.e. if the scalar product of the normals to the spacelike and timelike surfaces

¹³Usually one considers $M\beta = MT$ the action that an object of mass M would have if it had no entropy, so that the horizon contribution is only the constant part, $A/4$.

that meet does not vanish) has been shown by Hayward [20]. But in Euclidean spaces one must associate a finite action with joints, because these can be approached as limits of smooth surfaces. One must also introduce special rules about joints in adjacent regions so that the action is properly additive [21]: for example, two 90° corners, each with a positive value of $\int K$, can be put together to form a “ 180° corner,” i.e. no corner at all, and hence zero action contribution. In a sense the horizon area term in the action is a result of insisting on proper additivity of Euclidean actions with corners.

6.2 Tunneling Interpretation

Quantum mechanics allows a particle moving in a potential to tunnel into classically forbidden regions. The WKB wavefunction for such a particle can be obtained from the solution to a problem in classical physics, namely the motion of that same particle in imaginary time. Since the velocity is then imaginary, the kinetic energy is negative.¹⁴ The transition between real- and imaginary-time motion occurs at a classical turning point, where the particle’s momentum vanishes. At such a turning point the particle typically is most likely to be reflected, as predicted by classical theory, but there is a smaller probability that it makes a transition to imaginary-time motion until it finds another turning point, where it emerges as a classical particle in real time. Energy can be considered to be conserved during this whole motion. The tunneling probability contains an exponential factor, which can be computed from the action of the imaginary time (Euclidean) motion, and a prefactor, which can be computed from the motion of nearby particles. Although the Euclidean motion appears as a calculational device in quantum mechanics, it does trace out the “most probable escape path.”¹⁵

By analogy, Euclidean solutions of the Einstein equations represent such tunneling histories of geometries. In the metric representation of the (as yet unknown) quantum gravity, the wave functional Ψ depends on spacelike 3-geometries. A nearly classical Ψ is highly peaked about 3-geometries that all fit as embedded subspaces into *one* 4D spacetime. Conversely, a classical solution of the Einstein equations can be thought of as a representation of Ψ : You consider the 3-geometries of all the possible spacelike surfaces in the spacetime. Ψ is large on those 3-geometries, and vanishingly small on all others, that do not occur as subspaces of the given spacetime. A Euclidean 4-space can be considered in a similar way as a description of a Ψ that is large on all 3-geometries that fit into that Euclidean 4-space, and small on all others. Such wave functionals describe classically forbidden transitions, for example topology change. As for the particle, the beginning and end of the Euclidean motion occur at initial data of vanishing momentum, i.e. of vanishing extrinsic curvature (time-symmetric surface in the connecting Lorentzian spacetime). Such 3-geometries are the only ones that can satisfy both the Lorentzian and the Euclidean constraints, and are therefore suitable surfaces for signature change. Euclidean geometries that describe a transition to a real, Lorentzian spacetime (rather than just a virtual fluctuation) must have such a surface of symmetry, usually called the “bounce.”¹⁶

Many instantons correspond to a classically stable initial state, for example the vacuum, a classical background, or “nothing.” For a particle at the stable position $x = 0$ in a potential $V \sim x^2$, the Euclidean motion is an infinitely slow roll-off from the upside-down potential $V \sim -x^2$. Similarly, in an instanton geometry the initial state is found in the asymptotic region. To represent a transition the instanton must therefore have (1) the appropriate asymptotics (2) finite action I , so that the WKB factor e^{-I} in the transition amplitude is finite (3) a bounce

¹⁴If the total energy vanishes, the classical motion is the same as if the particle had the usual, positive kinetic energy, and the potential were turned upside down.

¹⁵One can measure the particle’s position along this path as long as the time remains ill-defined so that no large amount of energy is transferred to the particle.

¹⁶Other Euclidean solutions are called “instantons,” but this term is often also applied to bounce solutions.

surface of symmetry and (4) a finite prefactor. The prefactor is not easy to evaluate, so one usually is satisfied to show that it is finite. The essential property is that among the first order perturbations of the instanton there should be a “negative mode,” i.e. an eigenfunction of the action’s second order perturbation with negative eigenvalue. Thus one shows that there is a zero mode that has a node, which indicates that there is a lower, hence negative, eigenvalue.

The Euclidean Schwarzschild geometry is a typical example of a bounce solution. To see its properties, rotate Fig. 11 about an axis at $x = -2M$ as explained earlier, and look at a top view of the result, down the ρ -axis (Fig. 15). Each point in the plane at $r > 2M$ now represents a circle in the T -direction. At $r = 2M$ the circle degenerates to a point, and at $r < 2M$ there is a “hole,” no points in the Euclidean Schwarzschild geometry correspond to it. A possible bounce surface of symmetry is the equatorial plane; this is the final state of the tunnelling and the initial state of product of the transition. The geometry on this surface is given by the metric of Section 2 with $\theta = 0$. The initial state is in the asymptotically flat region, so it is a flat cylinder of topology $\mathbf{R}^2 \times S^1$.

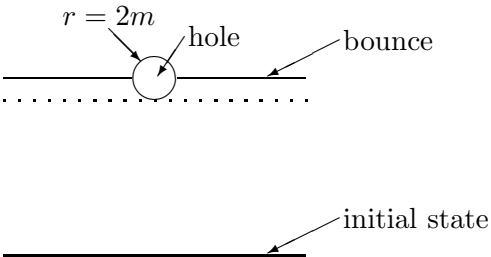


Fig. 15. The Euclidean Schwarzschild solution as a bounce, starting in the asymptotically flat region, developing to the surface (horizontal dotted line) where the hole first appears, and to the bounce surface where the curvature and the hole radius reach their maximum; followed by the symmetrical development back to flat space.

What physics does this bounce instanton describe? Its action (the Euclidean Schwarzschild action) is $< \infty$, as we saw. There is a zero mode — the active coordinate transformation of the metric that shifts everything in Fig. 15 rigidly upward. An infinitesimal shift has a node at the symmetry (bounce) plane. Hence there should be a negative mode, and the instanton describes a quantum transition of non-vanishing probability between the initial and the final state. The initial state is flat space, which is classically stable. It is somewhat strange because it is compact in one direction (the T -direction which, in spite of its name, is spacelike); but if we repeat the model one dimension higher, based on the 5-dimensional Schwarzschild solution, the initial state of type $\mathbf{R}^3 \times S^1$ can be interpreted as a Kaluza-Klein vacuum, compactified to length $\sim M$ in the extra direction. In either dimensionality the corresponding instanton connects the initial classical vacuum to a decay product, which starts its Lorentzian time development at the bounce surface with zero extrinsic curvature. The topology of the bounce surface is $\mathbf{R}^2 \times S^1$ for the 4D bounce, and $\mathbf{R}^2 \times S^2$ in the 5D case, so in the latter case a topology change is certainly involved. Its Lorentzian time development is another analytic continuation of the instanton metric, via $\theta \rightarrow i\theta$. The circular Euclidean hole becomes a hyperbolic timelike hole in the continuation, a hole that expands at constant acceleration in all directions. Thus the compactified vacuum is unstable to decay into an expanding hole, with the initial hole radius and its acceleration

determined by M , i.e. by the compactification scale [22]. Note that the actual decay history corresponds to only half of the bounce geometry, up to the bounce surface. Beyond that surface the signature changes and the Lorentzian development takes over.

Some instantons, when cut in half to reveal the bounce surface, have no other boundary or infinite region. These satisfy the Hartle-Hawking “no boundary” condition. In this case there is no initial state, which has been called “creation from nothing.” The simplest example is the S^4 Euclidean de Sitter solution, the round 4-sphere. An equatorial 3-space is the bounce moment, and the hemisphere which bounds it has no other boundary. In this view one can imagine the early history of the universe as in Fig. 15, a Euclidean “time-less” development of a bounce surface, where the signature changes to Lorentzian and de Sitter inflation starts.

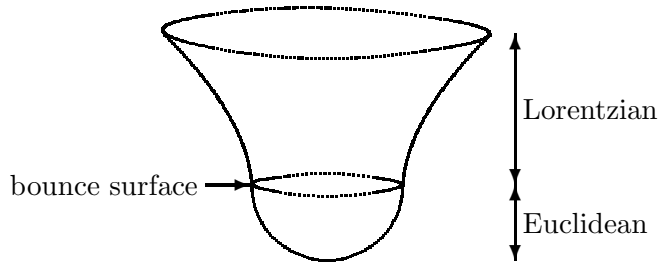


Fig. 16. The de Sitter universe created as a quantum event from nothing. It is tempting to think of the lowest point as the “nothing” from which the universe starts, but this has no invariant meaning, since the whole figure is invariant under the rotation/de Sitter group.

There are other universes that can be created from nothing if there is a cosmological constant, for example the Nariai universe. It is similar to the wormhole de Sitter universe (Fig. 7 with the two throats at R_o identified), except that it has the same size throughout (limit $R_o \rightarrow R_c$).¹⁷ However, the Euclidean action of these other universes is larger than that of de Sitter. They therefore contribute to the Hartle-Hawking state with a lower probability amplitude.

A very interesting set of instantons are those connecting a background field configuration with a bounce surface that contains a pair of black holes [23]. The background is a magnetic (or electric) field, and the instanton describes pair production of magnetically (or electrically) charged black holes by this field. This instanton metric is rather complicated, but a similar process occurs in — again — the de Sitter universe. Here the cosmological constant takes the place of the background field that pulls the virtual particles apart sufficiently to make them real. In fact, the Nariai solution mentioned above can be thought of in these terms, and the RNdS solutions provide other examples (where we must set either set $Q^2 = M^2$ to avoid Euclidean singularities, or use extremal black holes whose periodicity is arbitrary and can therefore be set equal to that of the cosmological horizon). Fig. 13 shows half of such a $Q^2 = M^2$ instanton, up to the bounce surface. It is a creation from nothing because there is no other boundary than the bounce surface, but in this case it is clear that there is no preferred point of “nothing” from which to start the universe. Note that not only the wormhole geometry but also its electric or magnetic field lines are created from nothing. The Euclidean action of these instantons has been calculated, so one can estimate the probability of the various outcomes (Nariai-type vs $Q^2 = M^2$ type vs extremal type, different M -values) relative to plain de Sitter space [24]. Generally the smaller the wormhole, the greater its probability.

There are also instantons that start from something rather than nothing, or vacuum, or background. These describe the type of quantum fluctuations often envisaged by Wheeler, whereby one extremally charged wormhole in asymptotically flat space breaks up into several

¹⁷This is similar to the limit discussed at the end of Section 3.

(or vice versa). The instanton [25] is analytically related to the Majumdar-Papapetrou solution for any number of extremally charged black holes, arbitrarily placed. This metric and field have the form

$$ds^2 = -V^{-2}dt^2 + V^2d\sigma^2 \quad A = V^{-1}dt$$

where $d\sigma^2$ is the metric of flat 3-space, and V is a solution of the Laplace equation in this 3-space, $\nabla^2V = 0$. To obtain the solution for several black holes in asymptotically flat space, one puts $V = 1 + \sum M_i/r_i$. But here we consider instead the Euclidean solution obtained by $t \rightarrow it$ and choosing a somewhat different V ,

$$ds^2 = V^{-2}dt^2 + V^2d\sigma^2 \quad V = \sum M_i/r_i \quad (10)$$

In the limit $r \rightarrow \infty$ this describes a cylindrical space of size $\sum M_i$, whereas in each limit $r_i \rightarrow 0$ we get a cylindrical space of size M_i . The instanton interpolates between these, as shown in Fig. 17.

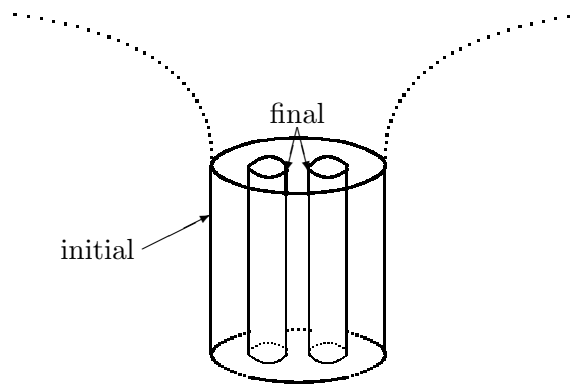


Fig. 17. Splitting of a Bertotti-Robinson universe into two, as an approximation of the splitting of an extremal Reissner-Nordström black hole. The dotted curve indicates the original black hole geometry, which approaches the Bertotti-Robinson geometry far down the throat. The t -direction of Eq (10) is plotted vertically. One angular direction is suppressed.

This is not a bounce instanton, because it is not cut in half by a bounce surface; it approaches the initial *and* final state asymptotically. It can therefore be regarded as describing a tunneling fluctuation, similar to the ground state in a double-well potential. The initial and final cylindrical geometries, when continued to Lorentzian spacetimes, are Bertotti-Robinson (BR) universes. Thus this instanton describes the splitting of such universes, but because the geometry deep down in the throat of extremal black holes approaches the BR geometry, it can also be regarded as a description of the splitting of an extremal black hole's throat.

The action of the instanton of Fig. 17 turns out to be entirely in the joints that the initial and final surfaces make with the horizontal surfaces. The interior does not contribute because the gravitational and electromagnetic contributions cancel (as is reasonable in a $Q^2 = M^2$ situation, where gravity is balanced by electromagnetism). The surfaces outside the joints have $K = 0$. The contribution of the j th joint is $A_j/16$, where A_j is the corresponding (horizon) area, and there are two joints for each horizon. Thus the total action is

$$I = \frac{\pi}{2} \left[\left(\sum M_j \right)^2 - \sum M_j^2 \right].$$

This action is independent of the axial length of the BR universes, or of the depth of the throats. It is also curious that I is half the difference of the entropies of the corresponding black holes (at

least according to one prescription for calculating this entropy). Thus the square of the WKB wavefunction e^{-2I} agrees with the probability $e^{\Delta S}$ associated in statistical mechanics with a fluctuation in which the entropy S deviates by ΔS from its equilibrium value.

7 The Multi-Black-Hole Solutions

Can analytic continuation from regular initial data lead to naked singularities? Cosmic Censorship forbids it, so one simple way to settle the question would be to find a counterexample. Consider, for example, the RNdS universe of Figs. 6 and 7. In this universe (as in the $\Lambda = 0$, asymptotically flat Reissner-Nordström (RN) geometry) a geodesic observer that wants to experience the singularity can do so, for example by moving along the vertical symmetry axis of the figure. In the RN case this is not considered a serious challenge to cosmic censorship, because the interior of the black hole, through which the observer in search of a singular experience must travel, is not stable under small perturbations of the exterior: radiation falling into the hole from the exterior would have a large blueshift at this observer — it would not only burn her up, but also change the nature of the singularity. It is remarkable that this does not necessarily happen in RNdS universes, for certain values of the parameters [9]. Thus these solutions are a counterexample to a strong interpretation of cosmic censorship. But there are, of course, many other geodesics that can lead observers who do not take the plunge to their safe haven at \mathcal{F}^+ .

For other parameters (the overmassive case) RNdS does have naked singularities: an observer at \mathcal{F}^+ in Fig. 9 sees them. But these singularities exist for all times, they do not arise from regular initial data. Can we find spacetimes with black holes that change from undermassive to overmassive? Progress on this question has been made possible by solutions of the Einstein-Maxwell equations that can describe merger of black holes.

A solution representing any number n of arbitrarily placed charged black holes in a de Sitter background is given by a metric of type (6), with a different potential U [1]:

$$ds^2 = -\frac{d\tau^2}{U^2} + U^2(dr^2 + r^2d\Omega^2) \quad U = H\tau + \sum_{i=1}^n \frac{M_i}{|r - r_i|} \quad A_\tau = \frac{1}{U}. \quad (11)$$

We will call this the KT solution. Each mass of the KT solution has a charge proportional to the mass, $Q_i = M_i$, and only the location r_i (not the initial velocity) is arbitrary. Here $|r - r_i|$ denotes the Euclidean distance between the field point r and the fixed location r_i in a Euclidean space of cosmological coordinates. For $n = 1$ this reduces to the $Q^2 = M^2$ case of the RNdS solution (6). Also, in the limit of large r , and for r_i in a compact region of Euclidean coordinate space, (11) approaches the RNdS solution with $M = \sum M_i$. One therefore expects the horizon structure at $r \rightarrow \infty$ to be similar to that of RNdS, which suggests that a $H > 0$ and a $H < 0$ version of (11) can be glued together as extensions of each other, similar to Fig. 8. The surprise is that, although this can be done with some degree of smoothness, it cannot be done analytically [11]. This means that there is no unique extension. An observer at rest in contracting ($H < 0$) cosmological coordinates, whose entire past can be described in these coordinates, has no way of telling what is in the other “half” of the de Sitter background (he can only guess that the total charge over there must be $-\sum M_i$, to balance the charge that he sees). If he moves and crosses the cosmological horizon $r = \infty$, the other, expanding half suddenly comes into view, seen at a very early time when all the masses are very close together. It is therefore reasonable that there is a pulse of gravitational and EM radiation associated with the horizon: this is the physical description of the lack of analyticity.

It is instructive to note how the various solutions differ in respect to possible coordinate choices. Pure de Sitter space has a static and two cosmological (expanding and contracting) coordinate systems centered about any timelike geodesic. In RNdS these coordinates are centered

about the black hole only, but one can still choose between expanding and contracting frames near either of the holes. In KT there is one set of black holes, all with the same sign of charge, that is uniquely expanding (the distances between holes increasing as $e^{H\tau}$), and another, oppositely charged set that is uniquely contracting (the distances decreasing as $e^{-|H|t}$). The expanding set is described by cosmological coordinates that include \mathcal{F}^+ , whereas for the contracting set, \mathcal{F}^- is included.

7.1 Merging Black Holes

Since black (as opposed to white) holes are determined from \mathcal{F}^+ , it is easiest to identify the black hole horizons for the expanding set. Consider the expanding coordinates in RNdS as in the left half of Fig. 7. The boundary of the past of \mathcal{F}^+ that lies in those coordinates is the left-hand line labeled $r = 0$ — it is the event horizon of the black hole in the “left” part of RNdS space. Similarly the event horizon of expanding KT space is given by $r - r_i = 0$. The Euclidean coordinate space with the n points r_i removed is a representation of \mathcal{F}^+ of expanding KT space. The n missing points represent n disjoint boundary components, and there is a finite distance between them at all times. Thus we have n black holes that remain separate for all times.

It is not as easy to identify the black holes in the contracting KT space, because that does not contain much of \mathcal{F}^+ . But because the cosmological horizon at $r = \infty$ is so similar to that of the RNdS space it does contain a “point” like S of Fig. 8 that is just enough to define the event horizon. So, to find the event horizon while staying within one coordinate patch we must find the surface that divides lightrays reaching $r = \infty$ from those that reach the singularity. But where in the KT world is the singularity? One can show that metrics of type (11) are singular where $U = 0$. In the contracting case, $H < 0$ (and of course $M_i > 0$), this happens only for positive τ . Thus we need to find the “last” lightrays that just make it out to $r = \infty$ at $\tau = 0$. More precisely (since $r = \infty$ is not a very precise place) we need $Hr\tau$ finite in this limit.¹⁸

If we know these last lightrays (the 3D horizon surface) we can then intersect them with a spacelike surface to find the shape of the 2D horizon at different times. An interesting question is whether this 2D horizon changes topology with time. This would, for example, describe the merger of two black holes into one. If black holes merge we can try to make an overmassive (hence nakedly singular) one from two undermassive ones, to test cosmic censorship. This is of course possible only in a contracting part of the KT solution, because we have already seen that the black holes in the expanding part remain separate for all times.

All contracting black holes do eventually merge into one. To show this for the case of a pair of holes, we show that the horizon must consist of two parts at early times, and be a single surface at late times. One can see rather directly that light starting at r sufficiently close to any one of the r_i at any time and in any direction will reach the singularity, because it will spend its entire history in a geometry sufficiently close to the single black hole, RNdS geometry. Thus points sufficiently close to r_i will always lie within the event horizon. So, for the case of two black holes, a key question is what happens to light that starts on the midplane between the holes. In fact, if the light starts early enough it will always be able to escape to $r = \infty$. Thus at early times the midplane does not meet the horizon — the two black holes are disjoint. To show this we center our Euclidean coordinates at the midpoint between the holes, which have a Euclidean separation d . From $ds^2 = 0$ in (11) we then find, for radial outgoing null geodesics in the midplane,

$$\frac{d\tau}{dr} = U^2 = \left(H\tau + \frac{M}{\sqrt{r^2 + d^2}} \right)^2 < \left(H\tau + \frac{\sqrt{2}M}{r + d} \right)^2.$$

¹⁸This is so because part of the “somewhat involved” coordinate transformation leading to (5) is actually rather simple, $R = Hr\tau + M$. For RNdS this is the static R , which is finite on the black hole horizon. Because near $r = \infty$ the KT geometry is so close to RNdS, R should also be finite for KT.

Now let

$$R_* = H\tau(r + d) \quad y_* = \ln(r + d)$$

to find

$$(r + d) dR_*/dr > R_* + H(R_* + \sqrt{2M})^2. \quad (12)$$

Standard analysis of this equation shows that if R_* is larger than the lower root of the RHS of (12), it will stay positive for all larger r . In terms of r and τ this means that if τ is sufficiently negative for any r (remember $H < 0$) then τ will remain negative as r increases — the lightray avoids the singularity. By a similar estimate one can show [11] that for each sufficiently late (but negative) τ there is a sphere surrounding both r_i such that all outgoing null geodesics will reach the $U = 0$ singularity. This means that the horizon surrounds both r_i , and the black holes have merged.

7.2 Continuing Beyond the Horizons

We could now discuss the merging of two undermassive into one overmassive black hole. Since the geometry near $r = \infty$ will be determined by the overmassive sum of the two individual masses, that neighborhood will look like the corresponding part of a single overmassive RNdS, that is, like the left hand side of Fig. 8. That contains a naked singularity (the left multiply-crossed line), which has nothing to do with the black hole merger, because it is located at the opposite side of the universe. But this is the only place in the coordinate patch where a $U = 0$ singularity occurs. Our patch does not describe enough of the history of the interesting region, where $|r - r_i|$ is small, just as the thick outline does not extend far to the right side of Fig. 8. To find out whether black hole merger generates its own naked singularity we must continue the KT metric beyond the inner black hole horizons at $r = r_i$. As we are continuing the KT geometry it is of course also interesting to look beyond the cosmological horizon at $r = \infty$, which exists only if the total mass is undermassive ($4|H|\sum M_i < 1$). So we look at null geodesics that approach these horizons.

Let us choose the origin $r = 0$ of our Euclidean coordinates at the location of the i^{th} mass (so that $r_i = 0$). The equation $ds^2 = 0$ satisfied by an ingoing null geodesic then takes the form, for small r ,

$$\frac{d\tau}{dr} = -U^2 = - \left(H\tau + \frac{M}{r} + \sum_{j \neq i} \frac{M_j}{r_j} \right)^2. \quad (13)$$

We can eliminate the last (constant) term on the right by defining a new time coordinate $\tau' = \tau + H^{-1} \sum' (M_j/r_j)$. The equation then becomes an equality version of (12), and by analyzing it in the same way as above one finds [11] the limiting forms

$$2H^2 r \tau' \rightarrow 1 - 2M_i H - \sqrt{1 - 4M_i H}. \quad (14)$$

To assess any incompleteness we need to know how a null geodesic $(r(s), \tau(s))$ depends on the affine parameter s , and we can get that from the variational principle,

$$\delta \int \left(-\frac{1}{U^2} \left(\frac{d\tau}{ds} \right)^2 + U^2 \left(\frac{dr}{ds} \right)^2 \right) ds = 0.$$

The Euler-Lagrange equation for $\tau(s)$ together with the first equality of (13) yields

$$\frac{d^2 r}{ds^2} - 2HU \left(\frac{dr}{ds} \right)^2 = 0.$$

Substituting (14) we find, in the limit $r \rightarrow 0$,

$$\frac{d^2 r}{ds^2} - \frac{1 - \sqrt{1 - 4M_i H}}{r} \left(\frac{dr}{ds} \right)^2 = 0$$

with the solution

$$r \sim (s - s_{\text{hor}})^{\frac{1}{\sqrt{1 - 4M_i H}}}, \quad \text{hence} \quad \tau \sim (s - s_{\text{hor}})^{-\frac{1}{\sqrt{1 - 4M_i H}}}. \quad (15)$$

So the inner horizon is reached at a finite parameter value s_{hor} . Similarly one finds that the cosmological horizon is reached in a finite parameter interval,

$$r \sim (s - s_{\text{Hor}})^{-\frac{1}{\sqrt{1 + 4(\Sigma M_i)H}}}, \quad \tau \sim (s - s_{\text{Hor}})^{\frac{1}{\sqrt{1 + 4(\Sigma M_i)H}}}. \quad (16)$$

This behavior of the coordinates r and τ gives us important information about the differentiability and analyticity of the geometry near the horizon. We can first eliminate whichever of the two is infinite on a given horizon in favor of $\hat{R} = Hr\tau$, which is always finite on the horizon. The metric is then an analytic function of remaining, finite coordinates, so the Riemann tensor will also be analytic in these coordinates. But in order that the geometry be differentiable, the Riemann tensor should be differentiable in the affine parameter s along null geodesics. Thus the differentiability of the geometry is measured by that of r resp. τ as a function of s , as given by (15) and (16).

Consider first the neighborhood of the inner horizon, where r is finite. Since $H < 0$ we have $1/\sqrt{1 - 4M_i H} < 1$, r is not a differentiable function of s at $r = 0$, and the Riemann tensor will be singular there. A more careful analysis [11], using a transformation to coordinates that are not singular on the horizon, shows that the metric is C^1 but in general not C^2 . There is therefore no unique, analytic extension across the inner horizon. One can match differentially essentially any KT solution with the same mass M_i . One can increase the differentiability by arranging the other masses carefully around the i^{th} one, so as to make the potential U approximately spherically symmetric (by eliminating multipoles to some order). The neighborhood of M_i then becomes approximately RNdS and hence “more nearly analytic” — i.e., of increased differentiability.

The situation near the cosmological horizon offers more variety. To have this horizon at all the total mass must be undermassive, $4|H|\Sigma(M_i) < 1$. Here τ is the finite one, and the corresponding power of s is $1/\sqrt{1 - 4(\Sigma M_i)|H|} > 1$. Thus τ is always at least C^1 . The transformation to coordinates that are good on the horizon shows that the metric is always at least C^2 . In the special cases when the power is an integer n , i.e., for masses such that

$$4H \sum M_i = 1 - \frac{1}{n^2},$$

the metric is C^∞ . For these values the smooth continuation matches the KT spacetime at the cosmological horizon to one with the same position and magnitudes of all the masses (so that all multipole moments agree), but with the opposite sign of H . We do not understand the physical significance of these special masses.

To show that the geometry at these horizons is not more differentiable than claimed one can compute the Riemann tensor. This infinity is of the null type mentioned in Sect. 2, and does not show up in invariants formed from the Riemann tensor. To see this for the horizon at $r = 0$ (or $r = \infty$) we write the metric (11) in terms of the coordinate $\hat{R} = Hr\tau$ and $y = \ln r$, and the quantity $W = rU$. Then the horizon occurs at $r \rightarrow \pm\infty$, where \hat{R} and W are finite,

$$ds^2 = -\frac{(d\hat{R} - \hat{R}dy)^2}{H^2 W^2} + W^2(dy^2 + d\Omega^2).$$

Now an invariant formed from the curvature tensor involves terms in derivatives of the metric and its inverse, multiplied by powers of the metric and its inverse. All these reduce to derivatives of W and \hat{R} divided by powers of W . But all derivatives of W remain bounded as $y \rightarrow \pm\infty$, and W is finite on the horizon. Thus the invariants cannot blow up.

Singularities do show up in the components of the Riemann tensor in a parallelly propagated frame, for example along the null geodesic $(r(s), \tau(s))$ discussed above. Let $l = \partial/\partial s$ be the parallelly propagated tangent. Because of the asymptotic symmetry near the horizon, $\eta = \partial/\partial\theta$ is also asymptotically parallelly propagated. Now the frame component $R_{\mu\nu\rho\sigma}l^\mu\eta^\nu l^\rho\eta^\sigma$ contains the term $g_{\theta\theta,ss}$. If $g_{\theta\theta} = W^2$ depends on r (and not just on the regular \hat{R}), it will not be a smooth function of s . In the RNdS (“single mass”) case, $g_{\theta\theta}$ depends only on \hat{R} . In the KT case the corrections to that behavior near an inner ($r = 0$) horizon start with the power $r^2 = (s - s_{\text{hor}}) \frac{2}{\sqrt{1-4M_i H}}$ unless there is special symmetry; thus one finds the differentiability of the metric as claimed above.

8 Naked Singularities?

Naked singularities visible to observers safely outside the strong curvature regions do not form in realistic gravitational collapse — this is the essential notion behind cosmic censorship. It can be made more precise in various ways [12]. At present none of these have been proved to be true in generic cases. When a proof seems difficult, it may be easier to obtain a convincing counterexample. Even if the conjecture is correct under certain assumptions, counterexamples are useful to test the necessity of these assumptions. For example, it may be that a version of cosmic censorship holds in pure general relativity, but fails when the theory is modified, say by a cosmological constant or by applying it to higher dimensions. There are in fact indications that cosmic censorship fails in the higher-dimensional theory inspired by string theory: certain 5D black strings (objects that appear four-dimensionally like black holes) are unstable, it is entropically favorable for them to decay into a set of 5D black holes, and during this decay naked singularities would form [13]. In the present contribution we want to test whether cosmic censorship fails in the special circumstances that are afforded when a cosmological constant is present.¹⁹

The idea of using KT spacetimes to test cosmic censorship is to start with two or more small (and hence not naked) black holes and let them collapse to form a single large (and maybe naked) one. We have seen that the KT solutions indeed can describe coalescing black holes, in the sense that the event horizons coalesce. But if it is possible to define the event horizon as we did, by observers who live for an infinite proper time in one KT coordinate patch, then these observers will see no signal from any singularity — all singularities that form from the initial data, including those in any of the (non-analytic) extensions, lie inside this event horizon. To find a situation where there is no “safe haven,” so that the generic observers does see a singularity, we must suppose that $\sum M_i$ is overmassive, so the initial black holes cannot be defined by their event horizon. An alternative to starting with black holes that have event horizons is to start with regular initial data on a compact surface. The KT solution cannot provide this either, because each M_i has an infinite throat. But such throats are the next best thing: each throat is undermassive, it is surrounded by a trapped surface, so one would not expect that the asymptotic regions down the throat could influence the solution in the interior. Can we, then, construct a KT solution of undermassive throats that has regular initial data and a naked singularity in its time development?

¹⁹A similar test for Einstein-Maxwell-dilaton theory with a cosmological constant inspired by string theory has been discussed in [14].

To decide this we must explore the global structure of the KT geometry. Unfortunately this cannot be completely represented by 2D conformal diagrams, because there is insufficient symmetry to suppress the additional dimensions. If we confine attention to the case of two equal masses, they lie on a line in the Euclidean coordinate space (which is an axis of symmetry of the spacetime). We can represent the essential features of the spacetime by drawing the conformal diagram for the spacetime spanned by the part of the axis going from one of the masses to infinity. This is shown in Fig. 18a. The part of the diagram representing the region near $r = \infty$ is to be read like a normal conformal diagram (i.e., each point represents a 2-sphere), whereas the region near $r = 0$ is to be thought of as doubled (each point represents two 2-spheres).

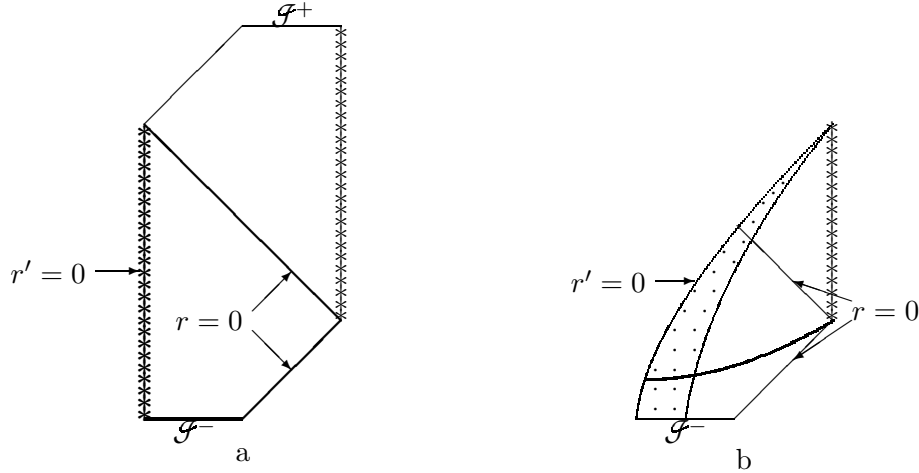


Fig. 18a. Conformal diagram of history of axis from one black hole to “infinity” for a two-black-hole contracting KT geometry. The black holes correspond to the region on the right, and the surrounding “de Sitter background” is the region on the left. The total mass is assumed to be overmassive, so this “background” is really an overmassive RNdS geometry with the singularity shown on the left. Therefore the axis extends to $r = \infty$ only for $\tau < 0$, after that it hits this singularity at $U(r, \tau) = 0$. The C^1 extension across the upper $r = 0$ horizon was chosen to be the time-reverse of the heavily outlined region.

Fig. 18b. In this diagram the cosmological singularity of Fig. 18a is covered up by a sphere of dust, as discussed in Sect. 4.1. The dust region is shown dotted. The thick curve is a spacelike surface with nonsingular initial data, containing two infinite charged black hole throats and, on the antipodal point of the universe, a collapsing sphere of dust. All observers have to cross the future $r = 0$ Cauchy horizon and can thereafter see the naked singularity shown on the right, the result of the merger of the two black holes. The spacetime ends after a finite proper time in a “big crunch.”

The region near $r = \infty$ of a KT solution (11) always behaves like an RNdS geometry with mass equal to the total mass $\sum M_i$. If this is overmassive, there will be a curvature singularity in this region, whether the individual (undermassive) holes have merged or not. This singularity at the antipodal point of the universe has nothing directly to do with the black hole merger. To obtain nonsingular initial data we can eliminate this singularity by replacing it with a collapsing sphere of dust, as in Sect. 4.1. The resulting diagram is shown in Fig. 18b. The initial data induced on the spacelike surface shown by the thick curve are now nonsingular. In the time development shown, beyond the future Cauchy horizons $r = 0$, a curvature singularity appears. It comes in from infinity through the infinite throats of the merged black holes and spreads to $r' = 0$, i.e. to the antipodal point of the universe. The fact that the infinite throats are hidden behind trapped surfaces does not seem to be sufficient to prevent the singularity from coming “out of” the throat. Perhaps a less coordinate-oriented way of saying this is that all of space collapses down the throats, carrying all observers with it.

It is clear from the diagram that all observers originating on the initial surface will reach the Cauchy horizon, and if they extend beyond, they will see the singularity. We have seen that the Cauchy horizon surrounding a typical KT throat is not smooth, so that delicate observers may not survive the crossing. But by distributing several KT masses symmetrically about a given one, we can make that one as differentiable as necessary to ensure an observer's survival. So it is reasonable to conclude that cosmic censorship is violated in these examples.

The initial data in these examples already contain the black holes' infinite throats, and are not compact. Can we first form the black holes from collapsing dust, and then let them go through the above scenario? We have seen in Fig. 10 that we can have simultaneous collapse of a dust ball to form a black hole, and simultaneously remove the overmassive singularity at the antipodal point by another dust ball. The problem is now that in the KT solution, as in the RNdS case shown in Fig. 10, the two balls collide before any singularities have formed, at least if the balls move on $r = 0$ resp. $r' = 0$ trajectories in KT (cosmological) coordinates. Even if we allow more general trajectories we know for charged test particles that the trajectories tend to avoid singularities of the same charge; and even if naked singularities were formed later in the evolution, one would not know whether they were a fundamental property of the theory, or due to the dust approximation ("shell crossing singularities," which occur also in the absence of gravity and hence have nothing to do with cosmic censorship).

Even if we accept the KT solution's infinite throats in place of compact initial data, we still do not yet have a serious violation of cosmic censorship, because the general KT solution is still quite special. The initial position and masses can be specified arbitrarily, but not the initial velocities. The constraints on the initial values can be solved in more general (but still not quite generic) contexts, for example one can drop the $Q_i^2 = M_i^2$ condition [11]. These initial data can be analytic, but we do not know what happens beyond the Cauchy horizon. In the general KT solution we have seen that one has to cross the Cauchy horizon to see the naked singularity. It is not clear whether more generic solutions have a Cauchy horizon with a stronger singularity than the KT solution. If so, then cosmic censorship would be preserved.

References

- [1] D. Kastor and J. Traschen, Phys. Rev. D**47** 5370 (1993)
- [2] P. Cruściel and J. Isenberg, Phys. Rev. D**48** 1616 (1993)
- [3] P. Cruściel and D. Singleton, Commun. Math. Phys. **147** 137 (1992)
- [4] K. Peeters, C. Schweigert and J. van Holten, *Extended Geometry of Black Holes*, preprint gr-qc/9407006
- [5] M. Walker, J. Math. Phys. **11** 2280 (1970)
- [6] K. Lake, Phys. Rev. D**20** 370 (1979)
- [7] B. Carter in *Black Holes* ed. C. DeWitt and B. DeWitt (Gordon & Breach 1973); D. Brill, Phys. Rev. D**46** 1560 (1992)
- [8] D. Brill and S. Hayward, Class. Quantum. Grav. **11** 359 (1994)
- [9] F. Mellor and I. Moss, Phys. Rev. D**41** 403 (1990) and Class. Quantum Grav. **9** L43 (1992); also see P. Brady and E. Poisson, Class. Quantum Grav. **9** 121 (1992); Brady, Núñez and Sinha, Phys. Rev. D**47** 4239 (1993); C. Chambers and I. Moss, Class. Quantum Grav. **11** 1035 (1994)

- [10] K. Lake Phys. Rev. D**19** 421 (1979)
- [11] Brill, Horowitz, Kastor and Traschen, Phys. Rev. D **49** 840 (1994)
- [12] See, for example, V. Moncrief and D. Eardley, Gen. Rel. Grav. **13** 887 (1981); R. Wald *General Relativity*, University of Chicago Press 1984; P. Joshi, *Global Aspects in Gravitation and Cosmology*, Oxford 1993 and the references cited there
- [13] R. Gregory and R. Laflamme, Phys. Rev. Lett. **70** 2837 (1993)
- [14] J. Horne and G. Horowitz, Phys. Rev. D**48** R5457 (1993)
- [15] J. A. Wheeler *Geometrodynamics*, Academic Press 1962
- [16] L. Romans Nucl. Phys. **B383** 395 (1992)
- [17] Banks, O’Loughlin & Strominger, Phys. Rev. D **47** 5370 (1993)
- [18] G. Ellis and B. Schmidt, Gen. Rel. Grav. **8**, 915 (1977)
- [19] G. Gibbons and S. Hawking, Phys. Rev. D**15**, 2752 (1977)
- [20] G. Hayward, Phys. Rev. D**47**, 3275 (1993)
- [21] D. Brill and G. Hayward, Phys Rev. D**50**, 4914 (1994)
- [22] E. Witten, Commun. Math. Phys. **80** (1981) 381
- [23] D. Garfinkle and A. Strominger, Phys. Lett. **B256**, 146 (1991); Garfinkle, Giddings and Strominger, Phys. Rev. D**49**, 958 (1994); H. Dowker et al, Phys. Rev. D**49**, 2909 and **50**, 2662 (1994)
- [24] R. Mann and S. Ross, *Cosmological production of charged black hole pairs*, DMPTP/R-95/9, gr-qc/9504015.
- [25] D. Brill, Phys. Rev. D**46**, 1560 (1992)